The skull of *Sphenacodon ferocior*, and comparisons with other sphenacodontines (Reptilia: Pelycosauria)

by David A. Eberth

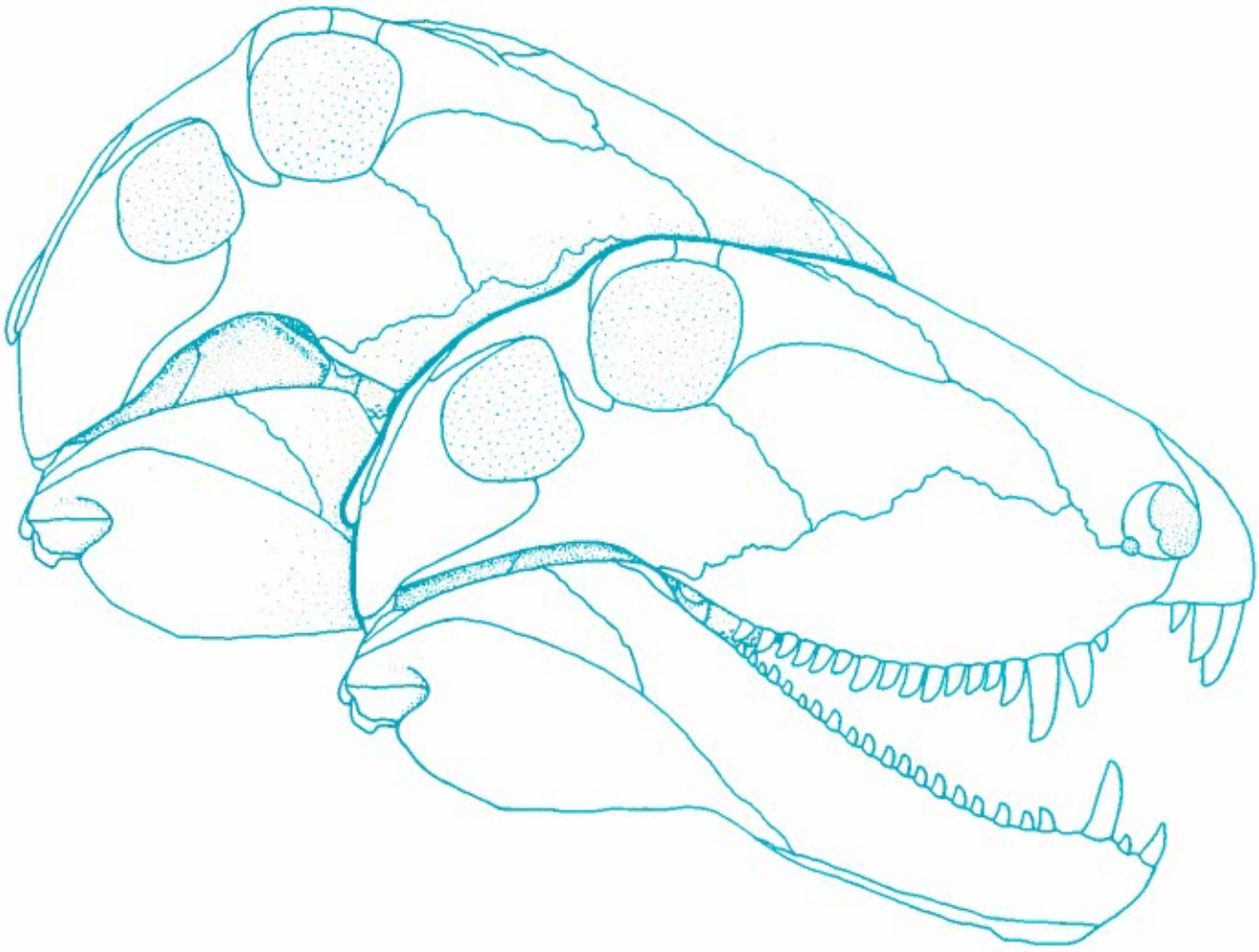

CIRCULAR 190 New Mexico Bureau of Mines & Mineral Resources 1985

A DIVISION OF

NEW MEXICO INSTITUTE OF MINING & TECHNOLOGY

Circular 190

New Mexico *Bureau* of Mines & Mineral Resources

A DIVISION OF
NEW MEXICO INSTITUTE OF MINING & TECHNOLOGY

The skull of *Sphenacodon ferocior*, and comparisons with other sphenacodontines (Reptilia: Pelycosauria)

by David A. Eberth

Department of Paleontology, University of California, Berkeley, California 94720

SOCORRO 1985

NEW MEXICO INSTITUTE OF MINING & TECHNOLOGY
Laurence H. Lattman, *President*

NEW MEXICO BUREAU OF MINES & MINERAL RESOURCES
Frank E. Kottlowski, *Director*
George S. Austin, *Deputy Director*

BOARD OF REGENTS
Ex Officio
Toney Anaya, *Governor of New Mexico*
Leonard DeLayo, *Superintendent of Public Instruction*

Appointed
Donald W. Morris, President, 1983–1989, *Los Alamos*
Robert Lee Sanchez, Secretary-Treasurer, 1983–1989, *Albuquerque*
William G. Abbott, 1961–1985, *Hobbs*
Judy Floyd, 1977–1987, *Las Cruces*
Steve Torres, 1967–1985, *Socorro*

BUREAU STAFF

Full Time

ORIN J. ANDERSON, *Geologist*
RUBEN ARCHULETA, *Technician I*
BRIAN W. ARKELL, *Coal Geologist*
AL BACA, *Crafts Technician*
JAMES M. BARKER, *Industrial Minerals Geologist*
ROBERT A. BIEBERMAN, *Senior Petrol. Geologist*
NANCY A. BLOUNT, *Coal Lab Technician*
LYNN A. BRANDVOLD, *Senior Chemist*
JAMES C. BRANNAN, *Drafter*
RON BROADHEAD, *Petroleum Geologist*
BRENDA R. BROADWELL, *Assoc. Lab Geoscientist*
FRANK CAMPBELL, *Coal Geologist*
RICHARD CHAMBERLIN, *Economic Geologist*
CHARLES E. CHAPIN, *Senior Geologist*
JEANETTE CHAVEZ, *Admin. Secretary I*
RICHARD R. CHAVEZ, *Assistant Head, Petroleum*
RUBEN A. CRESPIN, *Laboratory Technician II*
LOIS M. DEVLIN, *Director, Bus./Pub. Office*
NANETTE DYNAN, *Staff Secretary*
ROBERT W. EVELETH, *Mining Engineer*
ROUSSEAU H. FLOWER, *Sr. Emeritus Paleontologist*
MICHAEL J. HARRIS, *Metallurgist*
ZANA HARVEY, *Clerk-Typist*
JOHN W. HAWLEY, *Senior Env. Geologist*
CAROL A. HJELMING, *Editorial Secretary*
GARY D. JOHNPEER, *Engineering Geologist*
ANNABELLE LOPEZ, *Staff Secretary*
DAVID W. LOVE, *Environmental Geologist*
JANE A. CALVERT LOVE, *Assistant Editor*
WISS MALLDIN, *Driller*
VIRGINIA MCLEMORE, *Geologist*
LYNNE MCNEIL, *Staff Secretary*
NORMA J. MEEKS, *Department Secretary*
DAVID MENZIE, *Manager, Inf. Ctr.*
TERESA A. MUELLER, *Sci. Illustrator I*
DIANE MURRAY, *Geologist*
ROBERT M. NORTH, *Mineralogist*
GLENN R. OSBURN, *Economic Geologist*
JOANNE CIMA OSBURN, *Coal Geologist*
KATHRYN E. PARKER, *Drafter*
BARBARA R. POPP, *Biotechnologist*
MARSHALL A. REITER, *Senior Geophysicist*
JACQUES R. RENAULT, *Senior Geologist*
JAMES M. ROBERTSON, *Mining Geologist*
GRETCHEN H. ROYBAL, *Coal Geologist*
DEBORAH A. SHAW, *Assistant Editor*
WILLIAM J. STONE, *Hydrogeologist*
SAMUEL THOMPSON III, *Senior Petrol. Geologist*
MARK A. TUPA, *X-ray Technician*
JUDY M. VAIZA, *Executive Secretary*
MANUEL J. VASQUES, *Mechanic*
ROBERT H. WEBER, *Senior Geologist*
LINDA L. WELLS-MCCOWAN, *Drafter*
DONALD WOLBERG, *Vertebrate Paleontologist*
MICHAEL W. WOOLDRIDGE, *Chief Sci. Illustrator*
LISA ZANGARA, *Receptionist*
JIRI ZIDEK, *Chief Editor-Geologist*

Research Associates

CHRISTINA L. BALK, *NMT*
PAIGE W. CHRISTIANSEN, *NMT*
RUSSELL E. CLEMONS, *NMSU*
WILLIAM A. COBBAN, *USGS*
AUREAL T. CROSS, *Mich. St. Univ.*
JOHN E. CUNNINGHAM, *WNMU*
MARIAN GALUSHA, *Amer. Mus. Nat. Hist.*
LELAND H. GILE, *Las Cruces*
JEFFREY A. GRAMBLING, *UNM*
JOSEPH HARTMAN, *Univ. Minn.*
DONALD E. HATTIN, *Ind. Univ.*
ALONZO D. JACKA, *Texas Tech. Univ.*
DAVID B. JOHNSON, *NMT*
WILLIAM E. KING, *NMSU*
EDWIN R. LANDIS, *USGS*
DAVID V. LEMONE, *UTEP*
A. BYRON LEONARD, *Kansas Univ.*
JOHN R. MACMILLAN, *NMT*
HOWARD B. NICKELSON, *Carlsbad*
LLOYD C. PRAY, *Univ. Wisc.*
ALLAN R. SANFORD, *NMT*
JOHN H. SCHILLING, *Nev. Bur. Mines & Geology*
WILLIAM R. SEAGER, *NMSU*
JAMES E. SORAUF, *SUNY Binghamton*
RICHARD H. TEDFORD, *Amer. Mus. Nat. Hist.*
JORGE C. TOVAR R., *Petroleos Mexicanos*
LEE A. WOODWARD, *UNM*

Graduate Students

MARGARET BARROLL
GUNARS BERZIAS
JAMES T. BOYLE
LEE BROUILLARD
STEVEN M. CATHER
GERRY W. CLARKSON
TED EGGLESTON
CHARLES FERGUSON
GRANT GOODYEAR
ADRIAN HUNT
LAURA KEDZIE
RICHARD P. LOZINSKY
DANIEL MCGRATH
BRIAN E. MCGURK
WILLIAM MCINTOSH
JEFFREY MINIER
RICHARD REIMERS
STEWART SMITH

Plus about 50 undergraduate assistants

Original Printing 1985

Published by Authority of State of New Mexico, NMSA 1953 Sec. 63-1-4
Printed by University of New Mexico Printing Plant, January 1985

Available from New Mexico Bureau of Mines & Mineral Resources, Socorro, NM 87801

Contents

Figures

Tables

Abstract

Sphenacodon Marsh, known from the Lower Permian of New Mexico, Utah, and Arizona, is one of the best represented pelycosaurs in fossil collections, yet its skull has never been completely described. Virtually complete, disarticulated cranial remains of *Sphenarodon ferocior* from the Lower Permian Cutler and Abo Formations of north-central New Mexico are described in detail for the first time. These descriptions provide the basis for the most detailed comparisons to date within the genus *Sphenacodon* and the subfamily Sphenacodontinae.

No morphological differences exist between the skulls of *Sphenacodon* and *Ctenospondylus,* and only minor morphological differences exist between *Sphenacodon* and *Ctenospondylus* on the one hand and *Dimetrodon* on the other. On the basis of cranial morphology alone, *Sphenacodon* and *Ctenospondylus* appear to be more closely related than the current taxonomy reflects.

Macromerion is undiagnostic below the family level and materials referred to *Neosaurus, Bathygnathus,* and *"Oxyodon"* are undiagnostic below the subfamily level. The retention of all of these names except *"Oxyodon"* is recommended as a paleogeographic convenience. *"Oxyodon"* has been shown by Paton (1974) to be preoccupied, and pelycosaur material assigned to that taxon should be therefore reclassified as Sphenacodontinae incertae sedis.

Introduction

The Late Pennsylvanian to Late Permian subfamily Sphenacodontinae, as recognized by Romer and Price (1940) and Romer (1945), consists of seven genera *(Dimetrodon, Ctenospondylus, Sphenacodon, Bathygnatuss, Neosaurus, Oxyodon,* and *Macromerion).* Only three of these, *Dimetrodon, Ctenospondylus,* and *Sphenacodon,* include complete cranial remains. Known from the prolific Lower Permian red beds of Texas, Oklahoma, and New Mexico, *Dimetrodon* is represented by abundant skeletal material including numerous complete and partial skulls which have been thoroughly studied (Romer and Price, 1940). *Ctenospondylus* is represented by material from a number of different localities, which includes one articulated skull and postcranial material from southeast Utah, fragmentary cranial and postcranial remains from the Dunkard Group of West Virginia, and isolated spines and vertebrae pertaining to one individual from Texas. The cranial material from Utah was thoroughly studied and described by Vaughn (1964, 1969). The remaining cranial material from West Virginia was described and discussed by Berman (1978).

Sphenacodon, known from the Lower Permian Cutler and Abo Formations of New Mexico and the Cutler Group of Arizona and Utah, is one of the better represented pelycosaurs in North American fossil collections (second only to *Dimetrodon); yet, it* has received only a modicum of attention in the literature. Large collections of *Sphenacodon material* (cranial and postcranial) that were assembled by field parties from the Yale Peabody Museum in 1878, the University of Chicago and the University of Michigan in 1911, and the Harvard Museum of Comparative Zoology in 1937 have been the basis of virtually all the descriptions and figures of *Sphenacodon* cranial morphology (Marsh, 1878; Case, 1907; Williston, 1911, 1916, 1917, 1918; Case and Williston, 1913; Romer, 1937; Romer and Price, 1940). Unfortunately, much of this material is still in need of preparation, and that portion that has been prepared does not include a complete set of cranial elements. Thus, the cranial descriptions and figures are incomplete and somewhat patchy. *Sphenacodon* material collected by the University of California Museum of Paleontology during 1934 and 1935 was thoroughly prepared during the Work Project Administration years, and includes virtually every cranial element; yet, ironically, this material has never been described or figured. The reason for this neglect appears to have been the publication of the monumental *Review of the Pelycosauria* (Romer and Price, 1940). It has long been recognized that the skulls of *Sphenacodon* and *Dimetrodon* are very similar (Case, 1907; Williston, 1918; Romer and Price, 1940; Vaughn, 1964). Subsequent to the publication of the detailed descriptions and drawings of the articulated and associated cranial elements of *Dimetrodon limbatus in* the *Review of the Pelycosauria,* further interest in the cranial morphology of *Sphenacodon* and other sphenacodontines greatly diminished. Since 1940 most references to general sphenacodontine or sphenacodontid cranial morphology have been made by referral to the Romer and Price descriptions and reconstructions (e.g. Romer, 1956, 1966; Barghusen, 1968, 1973; Currie, 1979; Reisz, 1980; Brinkman and Eberth, 1983).

The University of California Museum of Paleontology *Sphenacodon* collection includes disarticulated, associated, and partially articulated skulls of no fewer than 31 individuals from one locality, as well as fragmentary and less abundant material from a number of other localities. Such a rich collection offers a unique opportunity to (1) provide the first in-depth, bonebybone description of a sphenacodontid, (2) examine variation in a sphenacodontine death assemblage, and (3) attempt an evaluation of intrasphenacodontine cranial variation. In the framework of Paleozoic reptilian systematics the description of this material is imperative. Much remains to be clarified concerning relationships of taxa within the Pelycosauria (Reisz, 1980; Brinkman and Eberth, 1983) and of pelycosaurs with other reptilian groups (especially therapsids). A thorough understanding of all pelycosaur genera is an essential step in addressing the nature of these

interrelationships. The University of California Museum of Paleontology *Sphenacodon* collection thus is thoroughly described in this paper. The goals are (1) to present a detailed, bone-by-bone description of the skull of *Sphenacodon* in the University of California collection, and (2) to provide cranial comparisons both within the genus *Sphenacodon* and among other sphenacodontines.

Acknowledgments

This study was undertaken at the Department of Paleontology of the University of California at Berkeley in 1979-81 as a partial fulfillment of a Master of Arts degree. I am greatly indebted to the late Dr. Malcolm J. Heaton of the Tyrrell Museum of Palaeontology, Alberta, Canada, at whose suggestion this study was initiated. Special thanks are due to Dr. Joseph T. Gregory who served as my thesis supervisor and critiqued earlier drafts of this paper. Drs. William A. Clemens and Harry W. Greene also read earlier drafts of this work, and I am grateful for their comments and observations. Drs. Robert R. Reisz and Donald Brinkman served as readers and provided many helpful comments and suggestions; both have been energetic sources of encouragement. Dr. P. P. Vaughn graciously allowed me to study and borrow the *Ctenospondylus cranial material* in his care. Research and travel were partially funded by monies from a University of California Regents Fellowship and the W. P. Schmidt Fund of the Field Museum of Natural History, Chicago. Field-work funds and publication expenses were generously provided by the New Mexico Bureau of Mines and Mineral Resources, Socorro, New Mexico. I am greatly indebted to Drs. Frank E. Kottlowski and Donald L. Wolberg of that institution.

Abbreviations

Institutional abbreviations used throughout this paper are as follows: UCMP, University of California Museum of Paleontology, Berkeley; MCZ, Museum of Comparative Zoology, Harvard University, Cambridge, Massachusetts; U.C., University of Chicago, Chicago, Illinois (this material is housed at the Field Museum of Natural History); WM, Walker Museum/ Field Museum of Natural History, Chicago, Illinois; NTM VP, Navajo Tribal Museum, Vertebrate Paleontology, Window Rock, Arizona.

Materials and methods

The genus *Sphenacodon* includes two species, the type species S. *ferox* (Marsh, 1878) and S. *ferocior* (Romer, 1937). The type of S. *ferox* is from the Lower Permian Cutler Formation, Baldwin bone bed locality in the village of Arroyo de Agua in Rio Arriba County, north-central New Mexico (Fig. 1; Langston, 1953, fig. 3). It consists of a single dentary and a pair of maxillae of questionable association. Other referred specimens of *S. ferox* have been collected from stratigraphically equivalent horizons throughout Arroyo de Agua and adjacent towns, from El Cobre Canyon 15 km northeast of Arroyo de Agua, and from the Johnson locality in the San Diego Canyon (see Langston, 1953).

S. ferocior is represented by articulated and disarticulated specimens that have been collected from localities of wider geographical extent than those containing *S. ferox.* The type of *S. ferocior* (MCZ 1489)—an articulated skull and partial postcranial skeleton—was collected from the Lower Permian Abo Formation in the San Diego Canyon, 2.5 km south of the Spanish Queen mine (Fig. 1; Langston, 1953, fig. 4). Referred specimens have been collected from localities in Arroyo de Agua that are stratigraphically 30-70 m higher than the Baldwin bone bed locality (Anderson and Cardillo quarries), throughout the San Diego Canyon (south of Jemez Springs) at stratigraphically higher positions than the S. *ferox* localities in that canyon, from the Abo Formation near Socorro in south-central New Mexico, and from the Organ Rock Shale of the Four Corners area (Vaughn, 1964).

Abundant, though fragmentary, remains of *Sphenacodon* sp. have been noted in the Permo-Pennsylvanian red beds of Socorro, San Miguel, and Santa Fe Counties in New Mexico (see Langston, 1952).

.Among all of these localities the Anderson quarry, in Arroyo de Agua, has produced the largest and most complete assemblage of disarticulated and articulated cranial remains of *Sphenacodon.* For this reason, and because most of the specimens were already prepared, *S. ferocior* from the Anderson quarry was chosen as the basis for the following descriptions and illustrations. At least 31 individuals are present and, in some cases, different ontogenetic stages of elements are represented. In most cases, elements are represented by more than one specimen, allowing for the study of variation in this death assemblage.

Five cranial elements are not represented in the Anderson quarry collection (tabular, vomer, supratemporal, ectopterygoid, and postparietal). The first two are described as they occur in the type (MCZ 1489). The supratemporal is known in an articulated, though crushed, skull of S. *ferox* (U.C. 35). It is described and figured as it occurs in that specimen. The postparietal is discussed with reference to its area of contact on the supraoccipital. The ectopterygoid is not discussed in any detail.

The specimen drawings are on coquille board. Outlines for each figure were obtained from enlargements

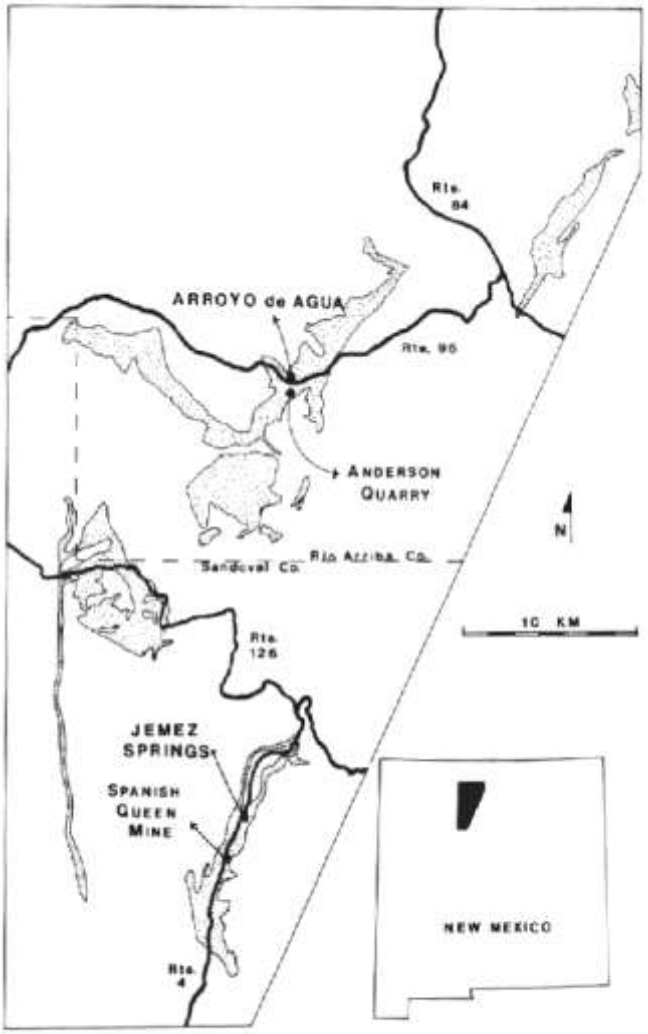

FIGURE 1—Locality map showing Lower Permian exposures in New Mexico (stipple) and *Sphenacodon ferocior* collecting localities discussed in this paper (Anderson quarry and Spanish Queen mine locality).

of photographic negatives projected directly upon the coquille board. Outlines of some of the smaller specimens were obtained directly from the specimen. Shading is present only where the element is preserved. In those cases where the full extent of the element can be reconstructed on the basis of evidence from adjacent elements, the reconstructed outline is dashed.

Reconstructions were only attempted where an articulated or obviously associated skull portion was available. The lateral-view reconstructions in Fig. 3A and B are based upon the articulated snout, UCMP 34196. Note that the cheek and temporal regions of the two reconstructions differ dramatically. The cheek region in Fig. 3A is based upon the jugal morphology present in UCMP 83208 (Fig. 14). The remainder of the temporal region in this reconstruction is an hypothetical reconstruction based upon disarticulated elements. The cheek region in Fig. 3B is based upon the jugal morphology in UCMP 34196. The remainder of the temporal and cheek region is an hypothetical reconstruction based upon an associated squamosal (UCMP 34196, Fig. 16) and other disarticulated elements. The lower-jaw reconstructions (Fig. 3C, D) are based upon a complete, articulated lower jaw, UCMP 83459. Insufficient articulated material was available to warrant an occipital, palatal, or dorsal reconstruction; thus, accurate measurements for these areas cannot be provided.

The sphenacodontines *Neosaurus, Macromerion,* and *"Oxyodon" are* in European collections, and, therefore, direct comparisons among these taxa, and between them and other taxa, could not be made. In these cases, comparisons are limited to those areas that have been described or figured by other authors. *Dimetrodon* specimens at the Harvard Museum of Comparative Zoology, a cast of the one known specimen of *Bathygnathus,* and the one known articulated skull of *Ctenospondylus* (NTM VP 1001) have all been examined first hand.

Locality and geology

The Anderson quarry is located in the village of Arroyo de Agua, Rio Arriba County, north-central New Mexico (SW 1/4 NW 1/4 Sec. 11, T. 22 N., R. 3 E.). In this area, deep valleys carved by erosive streams expose up to 200 in of sandstones and mudstones of the Cutler Formation (Fig. 2). Eight separate bone beds and numerous localities occur throughout the lower 100 m of this exposed section. Specimens that have been referred to *S. ferox* have been collected from the lowest six bone beds, all essentially at the same horizon (see Langston, 1952, 1953). The Anderson quarry bone bed occurs 60-70 m above these six lower bone beds. The quarry is exposed on the side of a small arroyo and includes an area of about 20 m². Bone-producing layers total approximately 1.5 m in thickness and the quality and quantity of preserved material is matched by few Permian localities. For the most part, the specimens are disarticulated, but when carefully extracted and prepared, elements are often fully preserved.

Environmental and/or taphonomic interpretations of the numerous bone beds in the Arroyo de Agua area have largely been avoided by workers concerned with systematics problems. Langston (1952, 1953), however, interpreted four of the lower bone beds as the discontinuously exposed remains of a large Lower

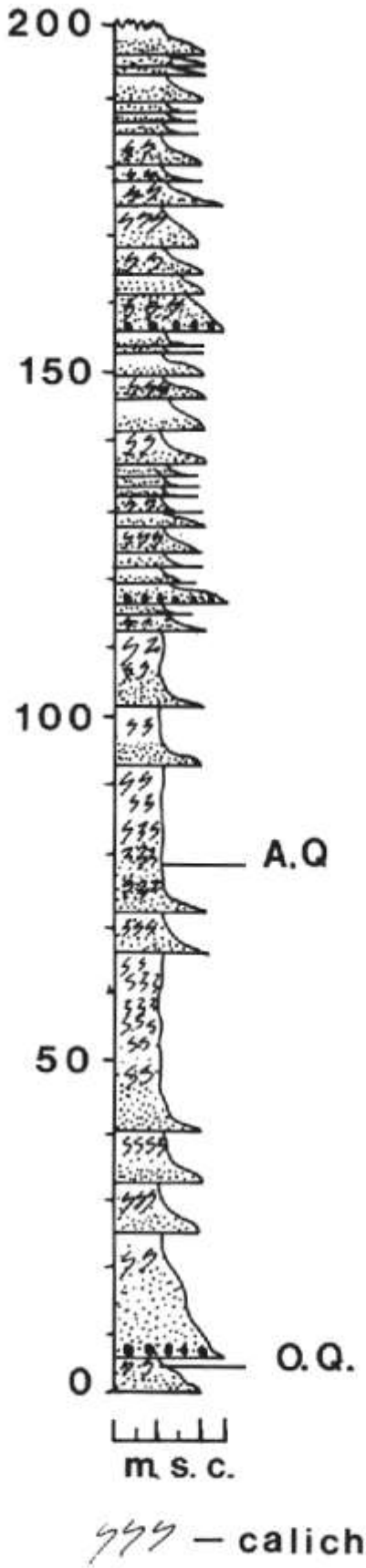

FIGURE 2—Cutler Formation (Lower Permian) lithologic section measured near Anderson quarry. A.Q., Approximate horizon of Anderson quarry; O.Q., approximate horizon of lower quarries containing *Sphenacodon ferox*.

Permian lake. He applied a similar interpretation to the higher-occurring Anderson quarry deposits, stating (1953, p. 360):

> . . . conditions of sedimentation were similar to those that produced the Welles quarry deposit, [one of the lower bone beds] but the chain of events was reversed and deposition took place nearer the shore. Repeated drying in the later history of the Anderson quarry lake is indicated by at least seven superincumbent marly layers in the upper 4 feet of the section.

Recent examination of this deposit has shown that the 1.5 m thick fossiliferous deposits occur as a laterally limited, U-shaped body containing three separate horizons. At the base a green-gray sandy silt rests unconformably upon a thick, multistoried sandstone body. This is overlain by a thin, nodular-rich marly horizon which, in turn, passes up into a thick, iron-rich marl horizon. The basal horizon is rich in carbonized plant material and produces the greatest variety of disarticulated, unassociated fossil remains. No obvious bedforms are preserved in any of these horizons.

The presence of a basal sandy-silt deposit containing abundant disarticulated and unassociated vertebrate remains and plant material suggests a complex transport history for this organic hash, followed by a quick burial. The overlying nodular-marl and iron-rich-marl horizons both contain the disarticulated and unabraded remains of larger tetrapods, often in association. Such information suggests the continued presence of a topographic low acting as a locus for pooling and maceration of carcasses. Although the U-shaped nature of these deposits speaks against their interpretation as remnant lake deposits, the lack of primary sedimentary structures makes any more definite interpretation difficult. It should be noted, however, that elsewhere in the section where laterally limited bodies of reduced sediments occur, their interpretation as the remains of proximal crevasse-channel fills is better documented (Eberth, in prep.).

The majority of the UCMP specimens collected from this deposit are from the lower two horizons. The upper marly horizon is very difficult to work and elements collected from it are often broken in the process of collecting. Although the lower two horizons undoubtedly represent two depositional events, rates of deposition and accumulation in environments where crevasse-channel deposits are forming today are very high (29-60 cm/100 yrs) (Smith, 1983). Thus, it is not unreasonable to consider the Anderson quarry *Sphenacodon* specimens as members of a single population.

Osteology

General osteology of the skull

The skull of *S. ferocior* (Fig. 3) is quite tall and narrow, with a long preorbital region and a short postorbital region. The bone of the snout is thin except at the alveolar ridges. The tooth row is convex in lateral view and the tooth bases are square in cross section, while the distal tips are compressed, with unserrated cutting edges along the anterior and posterior edges. Above the orbits the supraorbital ridge consists of thick bone and projects laterad, forming the widest portion of the skull table. A single temporal opening is present behind and slightly lower than the orbit. The occiput is a flat plate of bone inclined forward and set slightly anterior to the posterolateral corners of the skull. The stout paroccipital and supraoccipital processes brace the occiput against the posterior cheek region. Elongate internal choanae occur at the anterior end of the palate, adjacent to the thickened buttresses of the alveolar ridges. A wide, toothed, transverse flange of the pterygoid braces the posterior portion of the palate against the medial surface of the skull. Between these points the palate is covered with a shagreen of small, peg-like teeth arranged randomly in two fields along and on either side of the midline. Posterior to the transverse flanges, vertical processes of the pterygoids are sutured to the quadrates, thus forming stout braces between the occiput and the palate.

The lower jaw is quite narrow through most of its length and becomes thickened mediolaterad at the anterior end where the large caniniforms insert. The tooth row is concave in lateral view and the tooth morphology is as described above. Posterior to the tooth row, the mandible becomes tall and provides a large area for muscle insertion in the meckelian fossa on the medial surface. A meckelian canal runs forward from the fossa. Ventral to the fossa, the angular is a deep, narrow element. The condylar recesses of the articular are set just below the level of the tooth row and face dorsomediad. When the jaw is closed, the teeth of the lower jaw, with the exception of the caniniforms, come to lie medial to the maxillary teeth. The large caniniforms of the dentary are accommodated on the outside of the maxilla by a "step" formed along the anteroventral margin of the latter element.

Descriptions of cranial elements

Premaxilla (14 specimens)

The premaxilla, forming the blunt tip of the snout, is a tripartite, heavily ossified element that carries three teeth. Three processes contact the nasal dorsally, the maxilla and septomaxilla laterally, and the vomer and septomaxilla medially. The figured specimen (UCMP 83047) lacks only the tips of the three processes. Discussion of these regions is based upon the articulated partial skull, UCMP 34196.

The external surface of the bone is heavily pitted, as in most large reptiles, allowing an intricate set of blood vessels and nerves to communicate with the overlying skin. The first tooth is invariably the largest when compared to others in a fully erupted state. All the teeth are markedly ribbed in typical sphenacodont fashion. The roots of the first and second teeth are deeply implanted in the body of the premaxilla and, when fully erupted, extend up to the ventral border of the narial opening.

Arching posterodorsad for a distance of 4–4.5 cm from the body of the premaxilla, the dorsal process lies medial to the nasal and contacts the medial surface of its counterpart at the midline. This process, triangular in cross section, tapers dorsad, disappearing from the dorsal surface of the skull above and about 1 cm behind the posterior border of the narial opening. The sutural surface for the nasal lies along the lateral and posterior faces of the dorsal process. The midline sutural contact of the dorsal process (Fig. 4D) is in the vertical plane and is continuous with the medial sutural surface of the premaxillary body.

The slightly downturned maxillary process extends posteriorly 4-5 cm from the anterior border of the narial opening. It is sutured to the medial surface of the maxilla, terminating just above the "step" of the maxilla. The dorsal surface of this process is in contact with the footplate of the septomaxilla, although the full extent of this contact is not adequately indicated by the preserved material.

Extending posteriorly from the midline of the premaxillary body is the short, narrow, median process that marks the ventral contact of the nasal septum on the premaxilla. The medial and lateral surfaces of the process contact the anterior inner surfaces of the folded vomer. Only the medial sutural surface is visible, however. Between this short process and the maxillary process, which extends parallel to it, is a distinct furrow that may have carried a branch of the maxillary artery and perhaps the ethmoid nerve. Within this furrow, at a point directly behind the first-tooth root, is the prepalatal foramen. This opens into a vertical canal that in turn exits ventrally between the first and second teeth. The furrow continues forward entering the element at a point where the dorsal process begins to arch posteriorly from the body of the premaxilla (premaxillary foramen, Fig. 4B). Within the body of the premaxilla this foramen communicates with an extensive and complex series of canals. The manner in which these canals communicate with the surface of the premaxilla was determined by studying a series of 64 photographs taken from a serially ground specimen (UCMP 83033) at increments of 0.25 mm. It was determined that the posterior premaxillary foramen communicates with the root of the first tooth and continues as a large canal to emerge directly in front of the first tooth on the ventral surface of the premaxillary body. Throughout the course of this canal, smaller, anastomosing branches frequently run to the surface of the premaxilla. There is no evidence to suggest the existence of a single large sinus within the

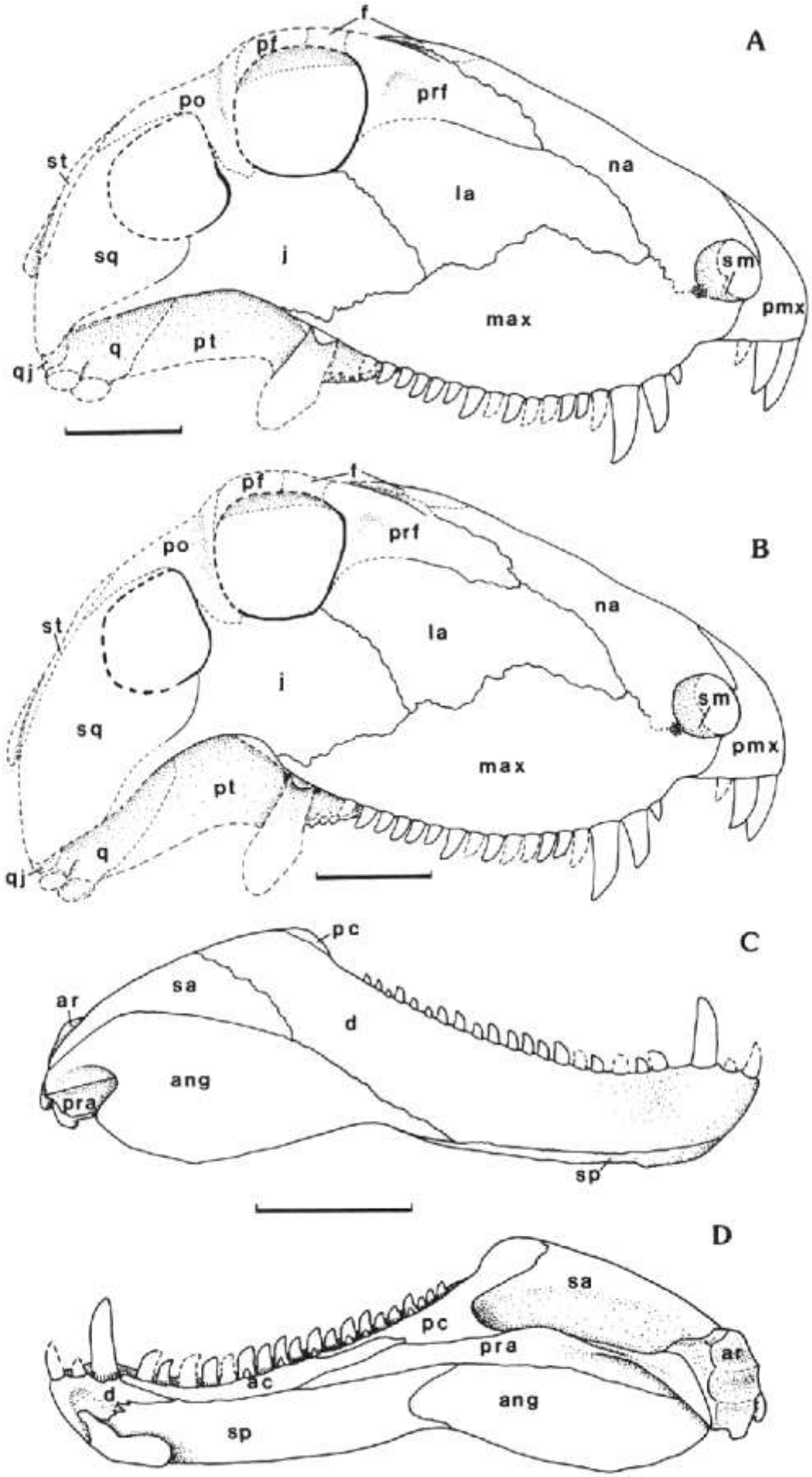

FIGURE 3—Two reconstructions of *S. ferocior* from the Anderson quarry: **A**, based upon UCMP 34196 and 83208; **B**, based upon 34196; **C** and **D**, based upon UCMP 83459. Note the difference in the angle of the posterior process of the jugal in A and B.

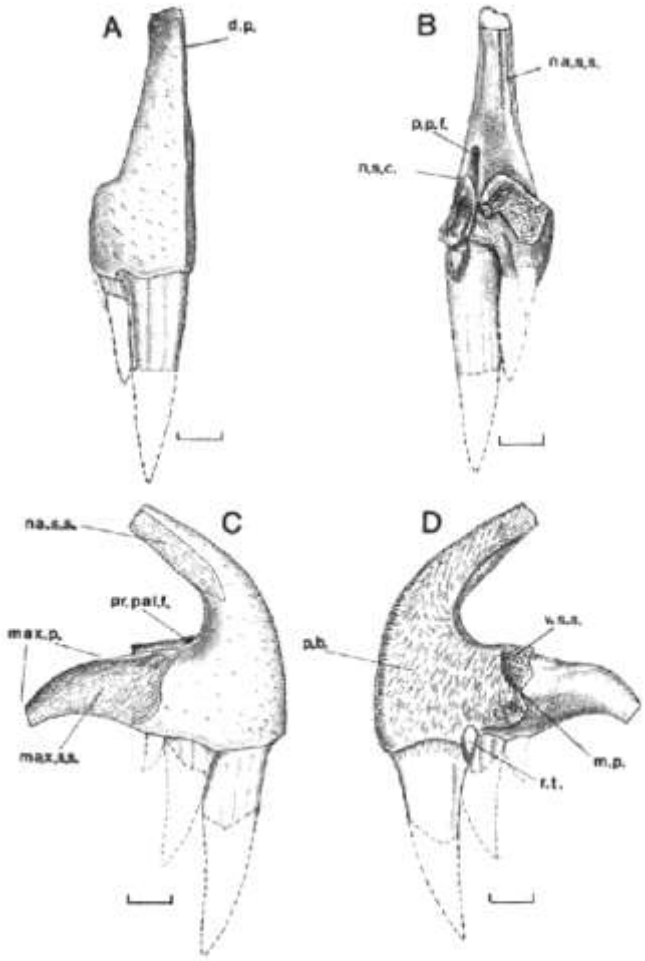

FIGURE 4—*S. ferocior*. Right premaxilla (UCMP 83047). **A**, anterior view; **B**, posterior view; **C**, lateral view; **D**, medial view. Abbreviations: **d.p.**, dorsal process; **m.p.**, median process; **max.p.**, maxillary process; **max.s.s.**, maxillary sutural surface; **na.s.s.**, nasal sutural surface; **n.s.c.**, nasal-septum contact; **p.b.**, body of the premaxilla; **p.p.f.**, posterior premaxillary foramen; **pr.pal.f.**, prepalatal foramen; **r.t.**, tooth root; **v.s.s.**, vomer sutural surface. Scale equals 1 cm.

dorsal process as seen in captorhinids (Heaton, 1979). The dorsal process remains cancellous throughout its length and appears to be similar in this respect to the dorsal processes of iguanids.

Septomaxilla (2 specimens)

The two available septomaxillae of *S. ferocior* are known from articulated, partial skulls and, in each case, have undergone a certain amount of distortion. UCMP 341% (Fig. 5A, B) shows the least distorted condition, but is poorly preserved anteriorly and medially. MCZ 1489 (Fig. 5C, D), on the other hand, is preserved anteriorly, but is compressed dorsoventrally, distorting the true nature of its contact with the nasal.

The septomaxilla provides protection for the anterior region of the nasal capsule and sits in the posterior margin of the narial opening, extending the full height of that orifice. The element is quite wide, extending from the lateral edge of the narial opening almost to the midline. It rests upon the medial and maxillary processes of the premaxilla. In medial view (Fig. 5B), UCMP 34196 appears as a gently convex structure firmly sutured to the internal surface of the nasal. A shallow groove runs along the ventral border of the nasal and ends in an area of crushed bone, preventing any attempt to trace its course. The groove marks the course of the lacrimal duct as it approaches the septomaxillary foramen, which is itself poorly preserved in this specimen. The area of crushed bone appears much too high to have been the region for the septomaxillary foramen and, more probably, represents the crushed posterior process of the septomaxilla that is applied to the internal surface of the nasal. The duct probably passed farther ventrad into the region behind the footplate. Even here, however, the presence of the septomaxillary foramen cannot be confirmed because of distortion. Anterior to this region of crushing, a light vessel scar branches ventrally.

In lateral view (Fig. 5A) only a small portion of the septomaxilla is visible; the anterior part of the element has been lost. The moderately sized septomaxillary foramen is clearly visible posteroventrally. A small portion of the medial shelf is preserved along the anterior edge. Below the shelf is a small, anteriorly opening foramen.

MCZ 1489, in contrast, shows the medial shelf well developed in either view (5C, D), but does not display a dorsal contact of the septomaxilla with the nasal. Along the ventral margin of the element, the footplate has lost its contact with the premaxilla. Thus, the septomaxilla appears curled up. In medial view (Fig. 5D) the septomaxillary foramen is visible and can be traced through to the external surface of the skull where it opens posterior to the footplate. The small anterior foramen seen in UCMP 34196 is not visible in any view, and the lacrimal duct scar leading to the septomaxillary foramen is not preserved. However, MCZ 1489 does show a completely preserved contact of the posterior process of the septomaxilla with the internal surface of the nasal (Fig. 5D).

Nasal (9 specimens)

The nasal is an elongate, gently arched element (Fig. 6A, B). At the anterior end the nasal sends a dorsal and a ventral process around the narial opening. The dorsal process contacts the lateral and the posterior surface of the dorsal process of the premaxilla along a narrow sutural surface. The ventral process extends some distance behind and beneath the narial opening and probably takes part in bordering the septomaxillary foramen dorsally. This process provides a broad ventral area of contact for the septomaxilla and maxilla on its medial surface.

The nasal is bounded laterally by the lacrimal and maxilla. In external view (Fig. 6B) the posterior part of the lateral edge shows a small sutural surface for the lacrimal. This surface is quite thin and is poorly preserved in all specimens.

The nasal tapers to a point between an anterior process of the frontal and the medial surface of the prefrontal (Fig. 6B). The medial edge of the element is thick through its entire extent. In medial view there

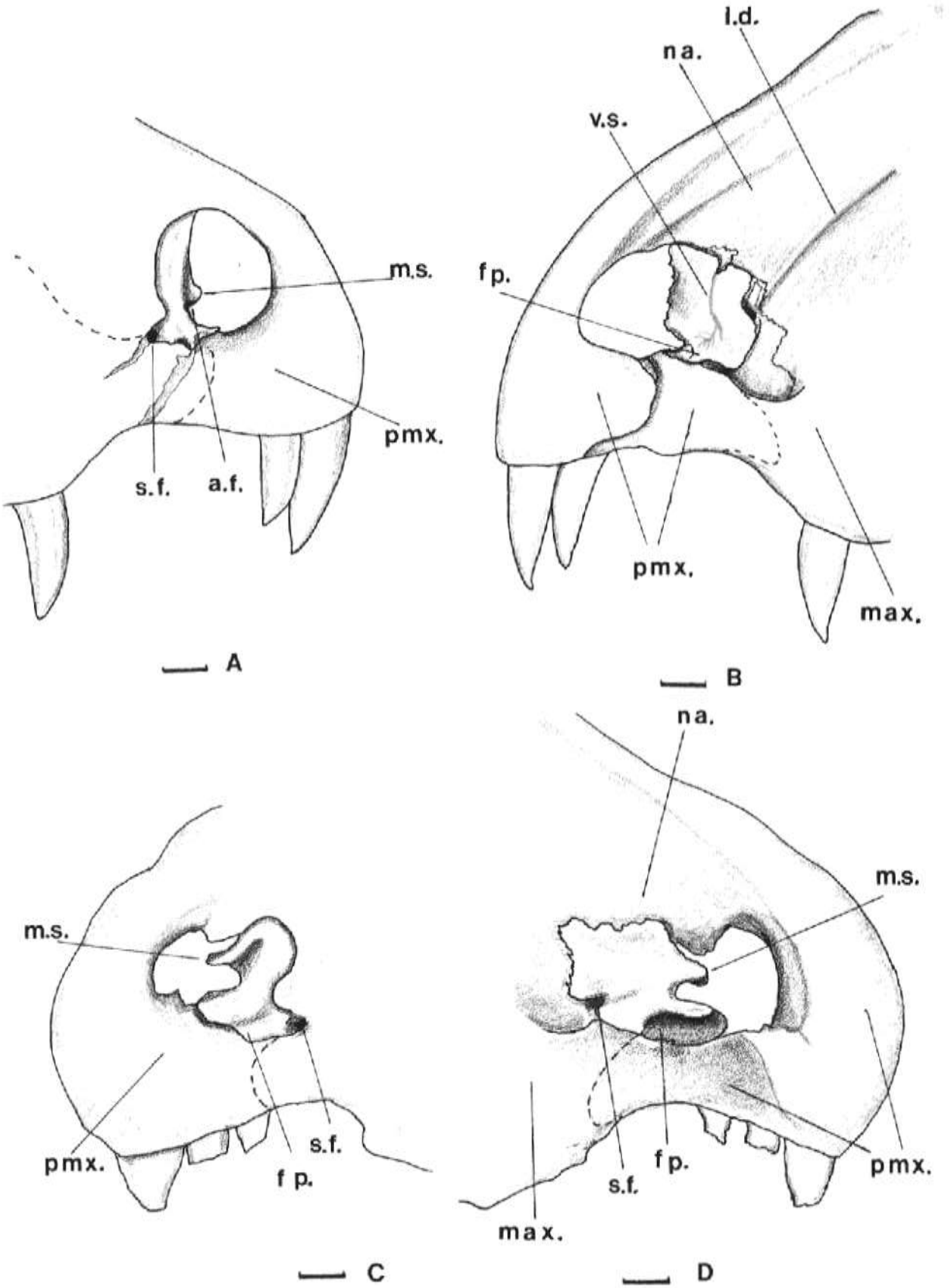

FIGURE 5—*S. ferocior*. Septomaxillae: **A**, lateral view of right septomaxilla (UCMP 34196); **B**, medial view of right septomaxilla (UCMP 34196); **C**, lateral view of left septomaxilla (MCZ 1489); **D**, medial view of left septomaxilla (MCZ 1489). Abbreviations: **a.f.**, anterior foramen; **fp.**, footplate; **l.d.**, course of lacrimal duct; **max.**, maxilla; **m.s.**, medial shelf; **na.**, nasal; **pmx.**, premaxilla; **s.f.**, septomaxillary foramen; **v.s.**, vessel scar. Scale equals 1 cm.

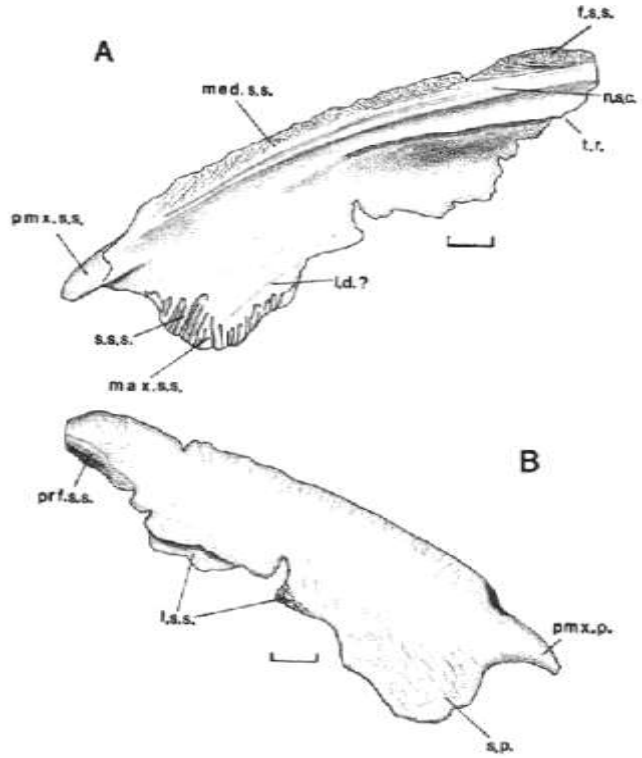

FIGURE 6—*S. ferocior*. Right nasal (UCMP 83203): **A**, medial view; **B**, lateral view. Abbreviations: **f.s.s.**, frontal sutural surface; **l.d.**, course of lacrimal duct; **l.s.s.**, lacrimal sutural surface; **max.s.s.**, maxillary sutural surface; **med.s.s.**, median sutural surface; **n.s.c.**, nasal-septum contact; **pmx.p.**, premaxillary process; **pmx.s.s.**, premaxillary sutural surface; **prf.s.s.**, prefrontal sutural surface; **s.p.**, septomaxillary process; **s.s.s.**, septomaxillary sutural surface; **t.r.**, turbinal ridge. Scale equals 1 cm.

is a narrow longitudinal groove, located lateral to the midline, that runs the length of the element. This possibly marks the point of attachment of the nasal septum. Lateral to this is a much wider, gently rounded groove that is well demarcated posteriorly. A similar groove has been hypothesized to mark the dorsal contact of the nasal septum in specimens of *Dimetrodon* **(Romer and Price, 1940). It is more likely that this groove results from the presence of a turbinal ridge lateral to it. Lateral to the turbinal ridge, the body of the nasal becomes thinner as it arches ventrolaterad. Along the medial surface of the element, just posterior to the narial border, is the light trace of a groove that is tentatively interpreted as the lacrimal-duct scar.**

Frontal (13 specimens)

The frontal is a triradiate, flattened element that consists of an anterior process, an orbital process, and a posterior process. The anterior process is long, narrow, and is convex dorsally when viewed laterally (Fig. 7A). It is structurally similar to the posterior region of the nasal with which it is continuous. A turbinal ridge extends forward along most of the ventral surface of the anterior process. The lateral surface of the anterior process displays sutural surfaces for the nasal and prefrontal. The prefrontal also contacts the frontal along the anterior edge of the orbital process, sending a small projection into the ventromedial corner formed between the anterior and orbital processes. The contact between the prefrontal and frontal extends forward to a point midway along the lateral surface of the anterior process of the frontal. At this point the two elements are separated by a posterior

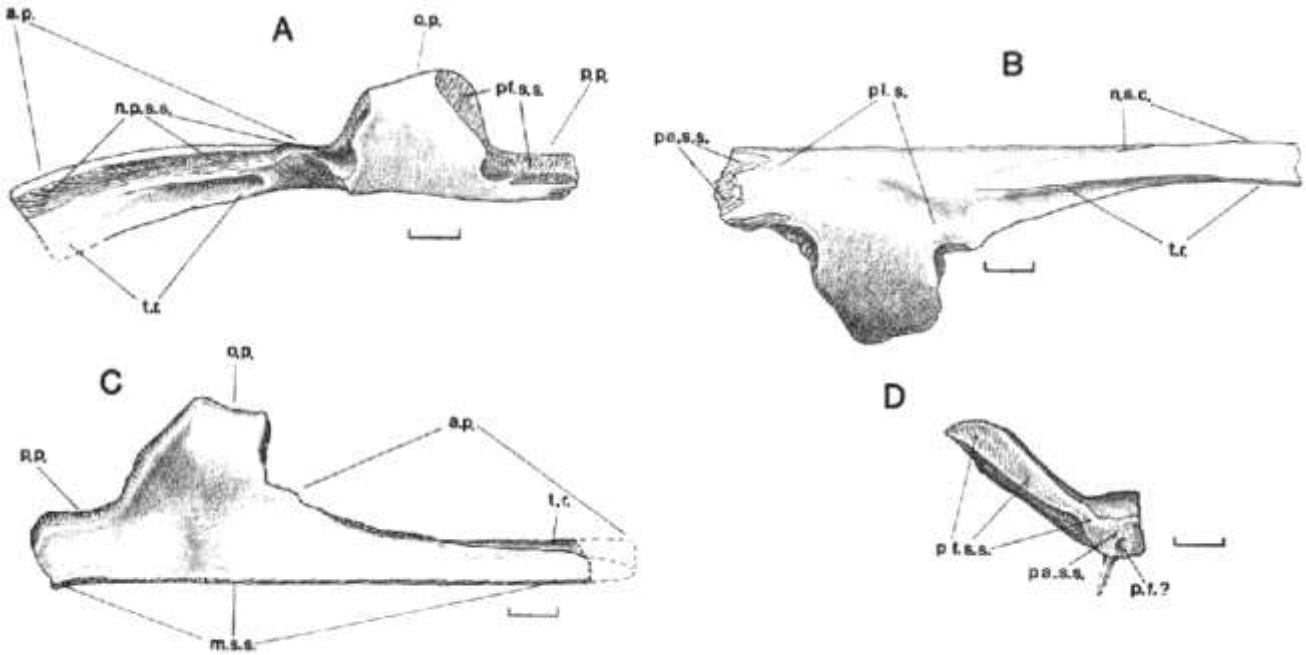

FIGURE 7—*S. ferocior*. Left frontal (UCMP 83193): **A**, lateral view; **B**, ventral view; **C**, dorsal view; **D**, posterior view. Abbreviations: **a.p.**, anterior process; **m.s.s.**, median sutural surface; **n.p.s.s.**, nasal–prefrontal sutural surface; **n.s.c.**, nasal-septum contact; **o.p.**, orbital process; **p.f.**, posterior foramen; **p.p.**, posterior process; **pa.s.s.**, parietal sutural surface; **pf.s.s.**, postfrontal sutural surface; **pl.s.**, planum supraseptale contact; **t.r.**, turbinal ridge. Scale equals 1 cm.

projection of the nasal. Williston (1925) indicated in his reconstruction of *S. ferox* that the nasal also projects posteriorly a short distance along the medial surface of the anterior process of the frontal. The articulated snout MCZ 1489 shows this condition to be present in *S. ferocior* as well.

The laterad projecting orbital process is dorsoventrally thick (7 mm) and forms the bulk of the supraorbital shelf. Along the posterior edge of the orbital process the sutural surface for the postfrontal is visible (Fig. 7D). The sigmoid curvature of the orbital process is visible in posterior view. The angle formed by the orbital process extending dorsolaterad from the midline is no more than 35° from the horizontal.

The posterior process displays an extensive area of contact with the postfrontal along its lateral surface. In ventral view (Fig. 7B), a shallow sutural scar marks the narrow contact of the parietal along the posteroventral surface of the posterior process of the frontal. In ventral view the frontal displays a small "step" that runs from the sutural scar for the parietal to the anteromedial corner of the orbital process. This marks the line of contact between the frontal and the dorsal extent of the planum supraseptale (solum supraseptale of Oelrich, 1956, and Heaton, 1979). Farther forward, a small ridge extends anteriorly, parallel to the turbinal ridge. This small ridge probably marks the line of contact between the nasal septum and the frontal. Between the anterior extent of the ridge marking the course of the planum supraseptale and the posterior portion of the turbinal ridge is a shallow depression that marks the posterior extent of the cartilaginous nasal capsule. The existence of a "pit" in this area, as noted by Romer and Price (1940) for *Dimetrodon*, is not present.

In posterior view (Fig. 7D) what appears to be a large foramen opens into the longitudinal axis of the frontal. The identity of this foramen is unknown.

Parietal (4 specimens)

The parietal is a small, wing-shaped bone at the posterior end of the skull table. The anterior surface of the element contacts the postorbital, postfrontal, and frontal. The posterior edge is in contact with the postparietal, tabular, and possibly the squamosal. The ventral surface is smoothly contoured, marking the limits of muscle attachments, and forms the dorsal roof of the braincase in the area immediately posterior to the pineal foramen. Fig. 8A, B presents reconstructions of the parietal based upon all of the available specimens.

Sutural surfaces for the postfrontal and frontal are visible in dorsal view (Fig. 8A). A large notch for the pineal organ occurs midway along the medial edge. In MCZ 1489 the pineal opening is just posterior to the midlength of the element, while in the three specimens from the Anderson quarry the notch occurs at about the midlength. On the posterior surface a large, forward-sloping sutural surface marks the contact of the postparietal and the tabular. The lateral wing of the parietal extends posteroventrad from the body of the element. Its dorsal surface is lightly striated, marking the anterior extent of the supratemporal.

In ventral view (Fig. 8B) the anterior and lateral edges of the wing are scarred by sutures marking the extent of postorbital contact. A narrow, scarred ridge runs along the posterior edge of the wing, marking the extent of the contact with the dorsal edge of the tabular. Sutural scars for the tabular along both the dorsal and ventral posterior edges suggest that the parietal was wedged into the dorsal edge of the tabular. From the material at hand it is impossible to determine the nature of contact between the parietal and the squamosal. Between the tabular and postorbital sutural scars a shallow, broad, concave surface

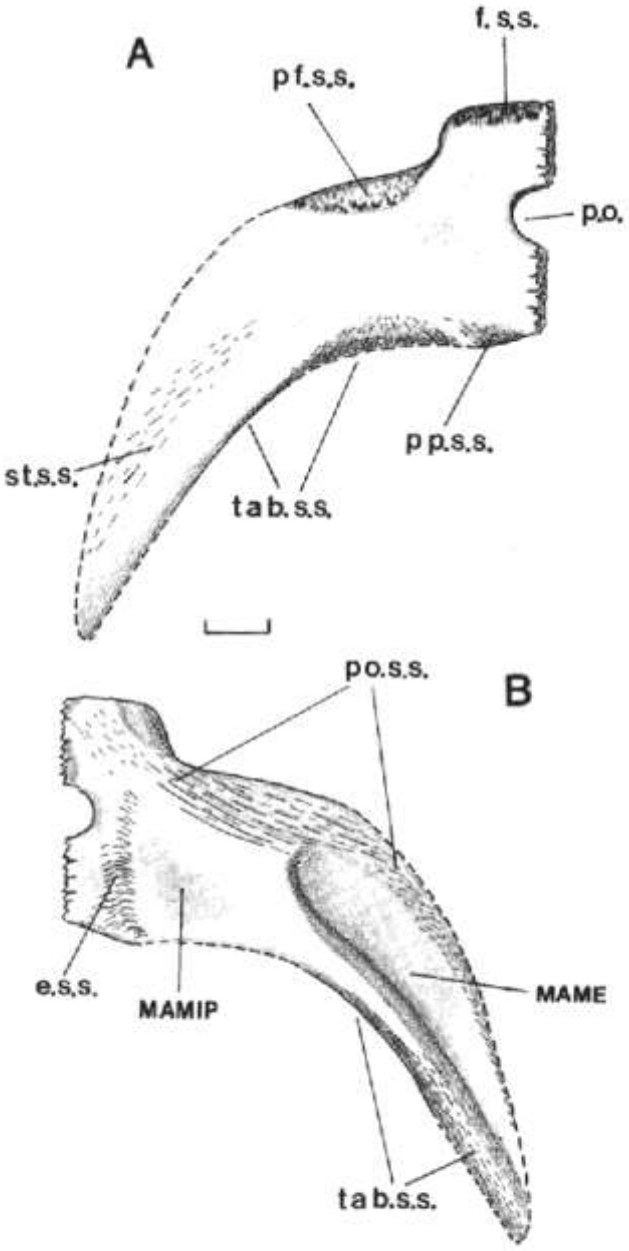

FIGURE 8—*S. ferocior*. Reconstruction of left parietal based upon UCMP 34194 and MCZ 1489: **A**, dorsal view; **B**, ventral view. Abbreviations: **e.s.s.**, epipterygoidal sutural surface; **f.s.s.**, frontal sutural surface; **MAME**, m. adductor mandibulae externus contact; **MAMIP**, m. adductor mandibulae (internal pterygoideus branch) contact; **p.o.**, pineal foramen; **pf.s.s.**, postfrontal sutural surface; **po.s.s.**, postorbital sutural surface; **pp.s.s.**, postparietal sutural surface; **st.s.s.**, supratemporal sutural surface; **tab.s.s.**, tabular sutural surface. Scale equals 1 cm.

that is heavily pitted around its periphery marks the site of attachment of part of the external adductor musculature. Medial to this area the parietal surface is softly contoured, possibly marking the site of attachment of the internal pterygoideus branch of the adductor musculature. Striae that occur along the ventral surface of the parietal, lateral to the pineal opening, might represent the contact point between the epipterygoid and the parietal, and thus the lateral limit of the braincase.

Postparietal (no specimens)

No isolated specimens of the postparietal exist in the UCMP Anderson quarry collection. However, much of the morphology of the element is known from sutural scars on the supraoccipital and the parietal.

Fig. 25A shows a posterior view of the supraoccipital with a large sutural-scar region for the postparietal. The element is apparently triangular, with its apex oriented ventrad. The limits and proportions of the postparietal can generally be deduced from these scars. The scars extend laterad to a point where the postparietal apparently overlies the medial edge of the tabular. Unfortunately, no sutural scars are preserved on the medial edge of the one fragmentary tabular used in this study (MCZ 1489) and, therefore, the exact lateral limit of the postparietal cannot be determined.

The supraoccipital abruptly contacts the posteroventral edge of the parietal, and the postparietal apparently covers this line of contact, extending dorsad onto the posterodorsal edge of the parietal.

Prefrontal (13 specimens)

The prefrontal bounds the anterodorsal area of the orbit, contacts the frontal and nasal along its narrow, dorsomedial edge, and broadly underlies the lacrimal ventrolaterally. No isolated prefrontals in the UCMP collection are preserved with the thin ventrolateral and anterior laminae that contact the lacrimal and nasal. The articulated snout UCMP 34196 was used to define the limits of these areas in Fig. 9.

The thick, posterodorsal orbital process forms the anterior portion of the supraorbital shelf. Anterior to the orbit a shallow fossa on the lateral surface of the element (Fig. 9A) marks an area of thin bone between the thickened orbital border and the medial edge.

In medial view (Fig. 9B) the thick orbital margin, triangular in cross section, appears continuous with the "step" on the ventral surface of the frontal that marks the contact between the frontal and the planum supraseptale. The ventromedial surface is lightly marked with striae. A complex sutural surface for the frontal and the nasal is visible along the dorsomedial edge of the prefrontal. Along the posterior half of the dorsomedial edge, the orientation of the sutural scars suggests an interdigitating contact with the frontal and the posterior half of the lateral edge of the nasal. Along the anterior half of the dorsomedial edge of the prefrontal, sutural scars indicate that the prefrontal overlies the ventrolateral edge of the nasal. The remainder of the medial surface of the prefrontal displays a number of thin, strut-like ridges running anteroventra d—posterodorsad.

Fig. 9C shows, in posterior view, the prominent interfingering sutural scar marking the extent of the contact with the frontal. Also visible in this view is the thickened orbital process. Two shallow grooves, possibly vessel scars, appear along the posterior surface of the bone.

Postfrontal (5 specimens)

The postfrontal is a thick, rectangular bone lying behind the frontal, with sutural surfaces on three sides and a rounded orbital margin on the fourth (Fig. 10). It strongly resembles the orbital process of the frontal and is frequently mistaken for that element in museum collections.

Sutural scars on the anterior face of the element (Fig. 10A) mark the contact with the posterior surface of the orbital process of the frontal. This contact continues around to the midpoint of the medial surface where it is supplanted by the sutural surface for the parietal. The latter continues onto the medial half of the posterior face of the postfrontal (Fig. 10C). The lateral half of the posterior surface is covered by a large, forward-inclined, postorbital sutural scar (Fig. 10C, D). The orbital margin is thicker than the rest of the element and is convex-up in lateral view (Fig. 10B).

Postorbital (11 specimens)

The postorbital is a triradiate element that forms the posterodorsal border of the orbit. It is rarely found fully preserved; the posterior and ventral processes are often lost during collection.

Most sutural surfaces are visible in medial view (Fig. 11D). The posterior process, which is triangular in cross section, curves posteroventrad to rest upon

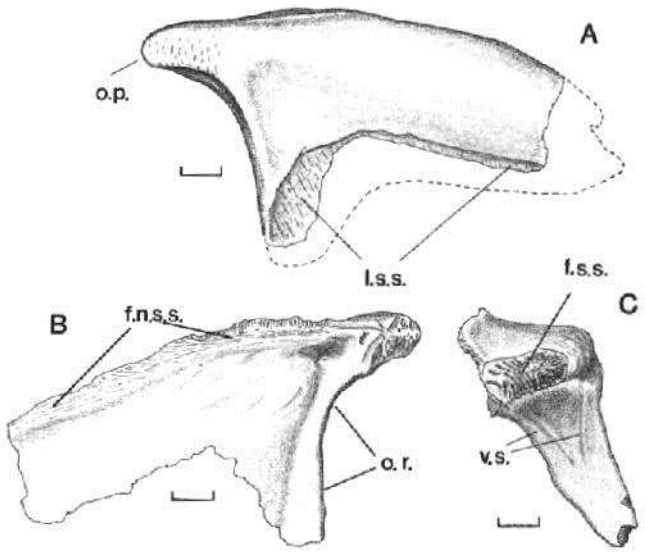

FIGURE 9—*S. ferocior*. Right prefrontal (UCMP 83185): **A**, lateral view; **B**, medial view; **C**, posterior view. Abbreviations: **f.n.s.s.**, frontal–nasal sutural surface; **f.s.s.**, frontal sutural surface; **l.s.s.**, lacrimal sutural surface; **o.p.**, orbital process; **o.r.**, orbital ridge; **v.s.**, vessel scar. Scale equals 1 cm.

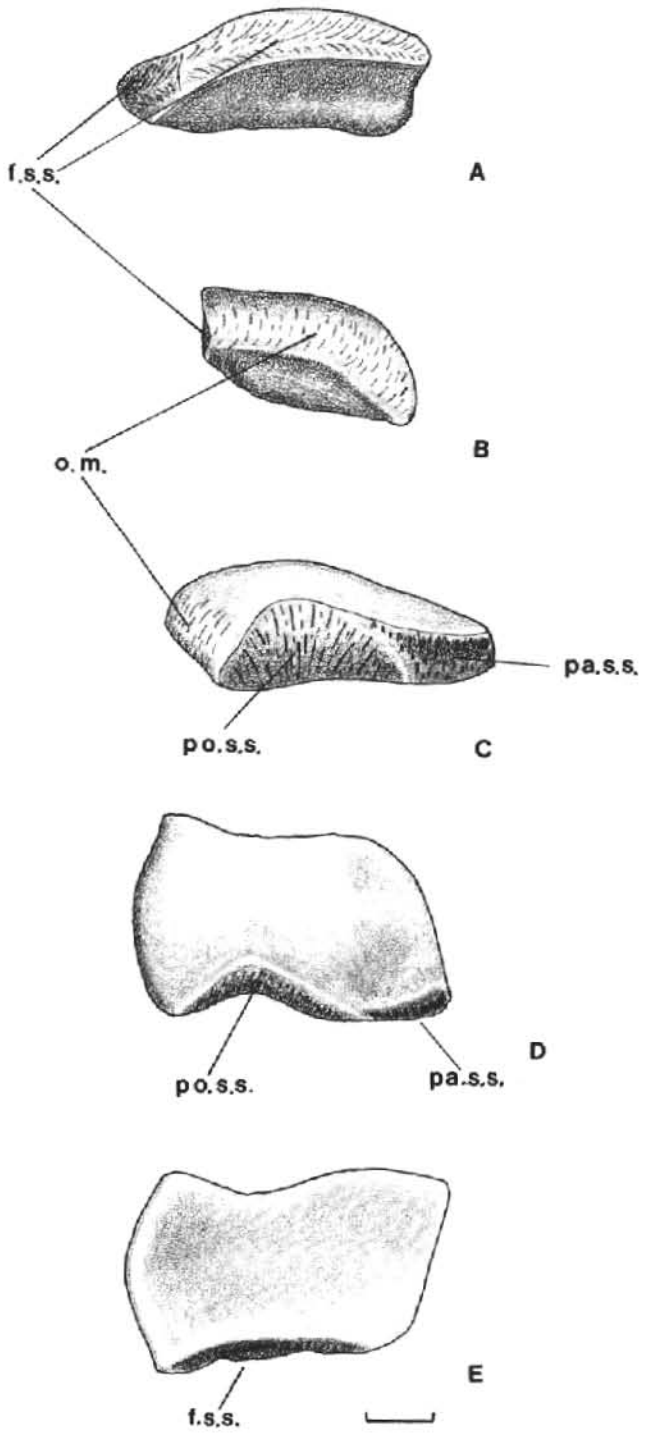

FIGURE 10—*S. ferocior*. Left postfrontal (UCMP 34184): **A**, anterior view; **B**, lateral view; **C**, posterior view: **D**, dorsal view; **E**, ventral view. Abbreviations: **f.s.s.**, frontal sutural surface; **o.m.**, orbital margin; **pa.s.s.**, parietal sutural surface; **po.s.s.**, postorbital sutural surface. Scale equals 1 cm.

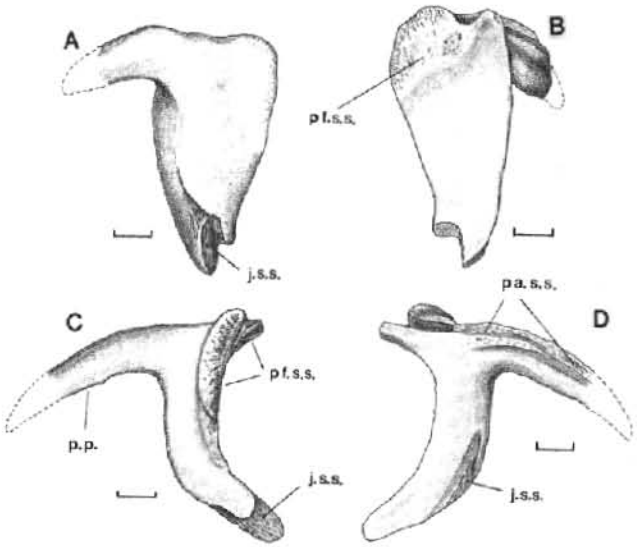

FIGURE 11—*S. ferocior*. Right postorbital (MCZ 1489): **A**, posterior view; **B**, anterior view; **C**, lateral view; **D**, medial view. Abbreviations: **j.s.s.**, jugal sutural surface; **p.p.**, posterior process; **pa.s.s.**, parietal sutural surface; **pf.s.s.**, postfrontal sutural surface. Scale equals 1 cm.

the posterodorsal surface of the squamosal. Reconstruction of the distal tip of the posterior process in Fig. 11 is based upon the morphology of the squamosal (UCMP 34196). The dorsal surface of the posterior process is deeply grooved for the anteroventral edge of the parietal wing. This groove continues forward onto the dorsal surface of the anterior process of the postorbital as well. The sutural surface for the postfrontal broadly covers the anterodorsal surface of the postorbital (Fig. 11B).

Together with the jugal, the ventral process forms the bar separating the temporal fenestra and the orbit. The jugal envelopes the posterior, lateral, and medial surfaces of the ventral process (Fig. 11A, C, D).

Maxilla (49 specimens)

The maxilla consists of a thickened, tooth-bearing alveolar ridge and a thin, vertical sheet of bone that extends dorsally from the lateral side of the alveolar ridge. The tooth row is markedly convex in lateral or medial view. The teeth are deeply implanted in a subthecodont manner (Romer, 1956, pp. 442–443). Romer and Price (1940) cited 14 teeth in the maxilla of the type of *S. ferocior* (MCZ 1489). Of the 12 complete tooth rows from the Anderson quarry available for study, total tooth counts range from 15 to 20 (Table 1). Although total tooth counts do not correlate well with stage of ontogenetic development, precaniniform tooth counts are, on the whole, greater in the smallest specimens (juveniles) than in the larger specimens (subadults and adults). Concomitantly, postcaniniform tooth counts appear to be slightly greater in the larger specimens than in the smaller specimens. Thus, although total tooth counts show the same range of variation among different ontogenetic stages, the non-caniniform-tooth series moves posteriorly relative to the enlarged caniniforms in large subadults and adults. Such relative movement results in the accentuation of the diastema between the last premaxillary tooth and the first maxillary tooth.

Most of the sutural surfaces are visible in medial view (Fig. 12A). The premaxillary process of the maxilla is deeply scarred, indicating the extent of the premaxilla's contact. Posterior to this, the ventral edge of the maxilla curves ventrad to form a prominent "step" anterior to the caniniform teeth. In the known

TABLE 1—List of UCMP maxillaries and their tooth counts. Abbreviations: **R/L**, Right/Left; **Ad.**, Adult; **Sub.**, Subadult; **Juv.**, Juvenile; **C**, Complete; **I**, Incomplete.

UCMP Specimen No.	R/L	Age	C/I	Precaniniforms	Caniniforms	Postcaniniforms	TOTAL
34182 (18 fragmentary specimens)							
34195	R	Ad.	I	0	2	10+	12+
34195	L	Ad.	I	0	2	10+	12+
34196	R	Ad.	C	1	2	15	18
34218	R	Ad.	C	1	2	12	15
34218	L	Ad.	C	1	2	15	18
45895	L	Juv.	C	4	2	14	20
83048	R	Ad.	C	1 (2)?	2	15	18 (19)?
83049	L	Ad.	C	0	2	14	16
83050	R	Sub.	C	3	2	12	17
83051	R	Sub.	C	0	2	14	16
83053	R	Sub.	I	0	2	12+	14+
83054	R	Ad.	I	0	2	10+	12+
83055	R	Ad.	I	?	2	13+	15+
83056	R	Sub.	I	1	2	6+	9+
83057	R	Ad.	I	?	2	14+	16+
83058	R	Ad.	I	1+?	2	13	16 (+)?
83059	R	Sub.	I	1+?	2	12+	15+
83060	R	Ad.	I	1	2	14+?	17 (+)?
83092	L	Sub.	C	2	2	12	16
83093	L	Ad.	C	2	2	12	16
83094	L	Sub.	I	1+?	2	9+	12+
83095	L	Sub.	C	1	2	9+?	12 (+)?
83096	R	Ad.	C	1	2	14	17
83097	L	Ad.	I	1	2	12+?	15 (+)?
83098	L	Sub.	C	1	2	14	17
83099	R	Ad.	I	0	2	8+	10+
83100	L	Sub.-Juv.	I	3	2	3+	8+
83101	L	Ad.	I	1	2	11+	14+
83102	L	Ad.	I	?	2	11+	13+
83103	R	Ad.	I	?	2	9+	11+
83104	R	Sub.	I	?	2	14+?	16 (+)?

juveniles (UCMP 45895, Fig. 36; UCMP 83100) the "step" is poorly developed. Large subadults and adults display strongly developed "steps" (Fig. 36). It is hypothesized here that the reduction in precaniniform-tooth number and the development of a "step" are two ways in which to accommodate the large caniniform mandibular teeth during jaw closure.

Posterior to the "step" a smoothly contoured buttress receives the immense and deeply implanted roots of the two caniniform teeth. Although only one fully erupted caniniform tooth is present in many specimens, some do possess two caniniforms simultaneously. Posterior to the buttress the alveolar ridge contracts and becomes rectangular in cross section. Sutural surfaces for the palatine and jugal-ectopterygoid are visible along its medial face. The palatine contacts the maxilla above the second caniniform tooth and continues the contact posteriorly, expanding onto the dorsal surface of the alveolar ridge. The sutural scars for the jugal and ectopterygoid are indistinguishable and are limited to the medial surface of the

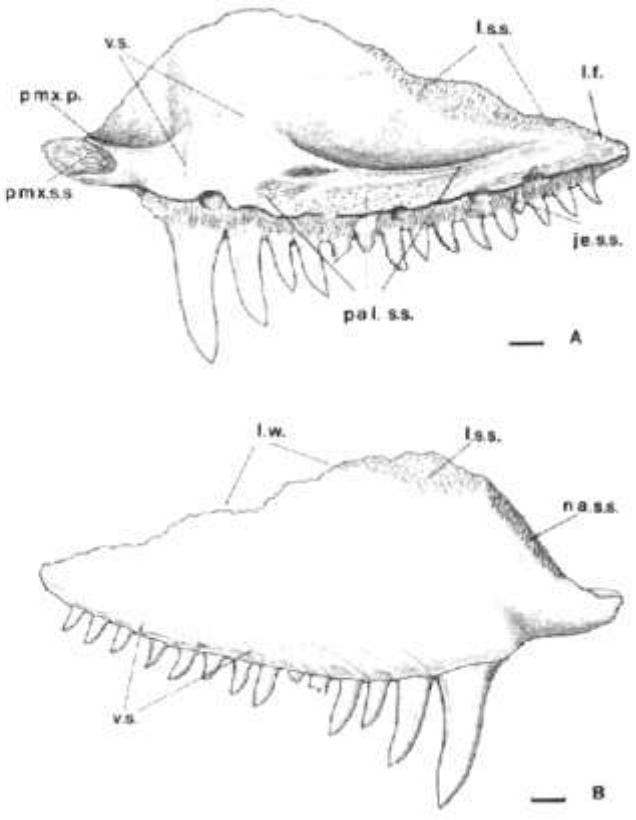

FIGURE 12—*S. ferocior*. Right maxilla (UCMP 83060): **A**, medial view; **B**, lateral view. Abbreviations: **a.r.**, alveolar ridge; **j.e.s.s.**, jugal-ectopterygoid sutural surface; **l.f.**, lacrimal-footplate contact; **l.s.s.**, lacrimal sutural surface; **l.w.**, lateral wall; **pal.s.s.**, sutural surface for palatine; **pmx.p.**, premaxillary process; **pmx.s.s.**, premaxillary sutural surface; **v.s.**, vessel scar. Scale equals 1 cm.

ridge. The lacrimal footplate gains contact in a shallow groove on the dorsal surface of the alveolar ridge, lateral to the palatine and above the last two maxillary teeth.

The nasal and a part of the lacrimal contact the lateral surface of the dorsal wall of the maxilla, along the anterior edge of the latter. The dorsal wall of the maxilla is thickened at the nasal sutural surface. The sutural surface for the lacrimal extends posteriorly along the lateral surface of the dorsal edge of the wall just behind the nasal sutural surface. The lacrimal sutural surface switches onto the medial surface posterior to the dorsal apex of the dorsal wall. It is not extensive and is superseded by a sutural surface for the jugal (Fig. 12A).

A vessel scar appears at midlength on the dorsal surface of the alveolar ridge and continues forward, up the caniniform buttress where it becomes visible in medial view (Fig. 12A). A foramen on the buttress marks the point where soft tissue entered that structure. The vessel scar continues forward over the buttress and, as it descends the anterior surface, bifurcates, sending another scar down the medial face. The anterior scar continues forward into the depression formed by the dorsal wall and the thickened lateral edge of the premaxillary process. It bifurcates again before reaching the anterior end of the maxilla.

The identity of the structures carried in these scars is not clear. It seems plausible that they were the rami of the maxillary artery and possibly the lateral palatine artery.

Lacrimal (3 specimens)

The lacrimal extends forward from the orbit as one of the thinnest and lightest dermal bones of the skull. Presumably because of its lightness and susceptibility to distortion and destruction, only two isolated specimens are known from the Anderson quarry.

In external view (Fig. 13A) the large jugal and smaller maxillary sutural surfaces are visible but not very distinct. The external surface of the bone is lightly scarred by blood-vessel tracks. A small portion of the element is exposed in the orbital margin and houses the opening for the lacrimal duct at its ventral edge. The lacrimal duct is small, with a diameter not exceeding 3 mm. The duct runs forward, opening on the inside of the element, 1-2 cm from the anterior edge of the element. The duct presumably continued forward closely appressed to the medial surface of the nasal, terminating at the septomaxillary foramen.

The dorsal edge of the lacrimal overlaps the nasal and prefrontal (Fig. 13B). The ventral edge overlies the anterior portion of the dorsal wall of the maxilla and underlies the posterior portion of the wall. The internal surface of the lacrimal is covered completely with a series of anteroventrad oriented ridges, one of which—the lacrimal footplate—has an extensive contact with the dorsal surface of the alveolar ridge of the maxilla.

Jugal (14 specimens)

The jugal is a flat bone that forms the ventral border of the orbit and temporal fenestra, and the ventrolateral border of the skull just posterior to the orbit.

In lateral view (Fig. 14A) the postorbital process ascends between the orbit and the temporal fenestra. The process is incised anteriorly to receive the jugal process of the postorbital. The posterior process of the jugal tapers posteroventrad. A few specimens possess strongly downturned posterior processes (e.g. Fig. 15B). Much of the lateral face of the posterior process is overlapped by the squamosal. Anteroventrally, the maxillary sutural surface appears as a narrow strip.

In medial view (Fig. 14B) an anteroventrad recurving ridge, triangular in cross section, originates on the postorbital process of the jugal and terminates as a blunt ventral projection just below the ventral edge of the body of the element. The medial surface of this blunt projection abuts against the dorsolateral corner of the transverse process of the pterygoid. Anterior to this, scars mark the broad sutural surface for the lacrimal. The **full** extent of this contact has been inferred from the morphology of the adjacent lacrimal.

A series of tiny pits and parallel ridges along the medial surface of the posterior process indicates a heavy concentration of nutritional foramina.

Squamosal (9 specimens)

The squamosal is a markedly three-dimensional bone with flattened lateral and posterior surfaces oriented at 90° to one another. In lateral view (Fig. 16A) the

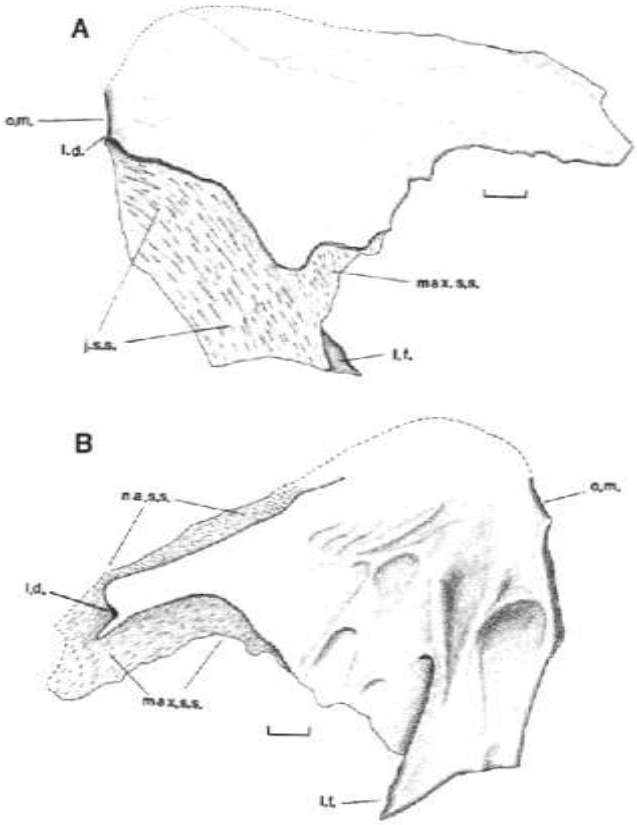

FIGURE 13—*S. ferocior*. Reconstruction of right lacrimal based upon UCMP 34196 and 34192: **A**, lateral view; **B**, medial view. Abbreviations: **j.s.s.**, jugal sutural surface; **l.d.**, lacrimal duct; **l.f.**, lacrimal footplate; **max.s.s.**, maxillary sutural surface; **na.s.s.**, nasal sutural surface; **o.m.**, orbital margin. Scale equals 1 cm.

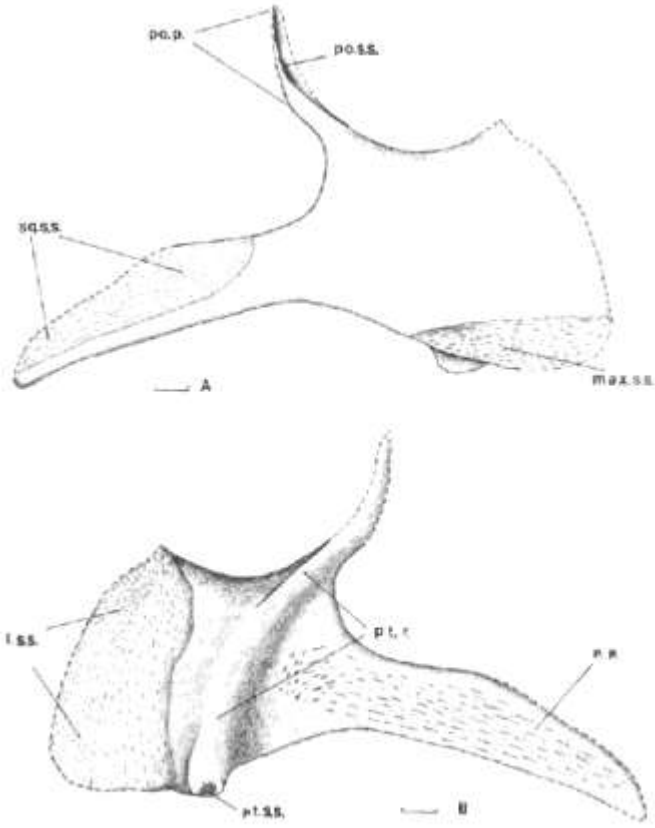

FIGURE 14—*S. ferocior*. Reconstruction of right jugal based upon UCMP 83208: **A**, lateral view; **B**, medial view. Abbreviations: **l.s.s.**, lacrimal sutural surface; **max.s.s.**, maxillary sutural surface; **p.p.**, posterior process; **po.p.**, postorbital process; **po.s.s.**, postorbital sutural surface; **pt.r.**, pterygoid ridge; **pt.s.s.**, pterygoidal sutural surface. Scale equals 1 cm.

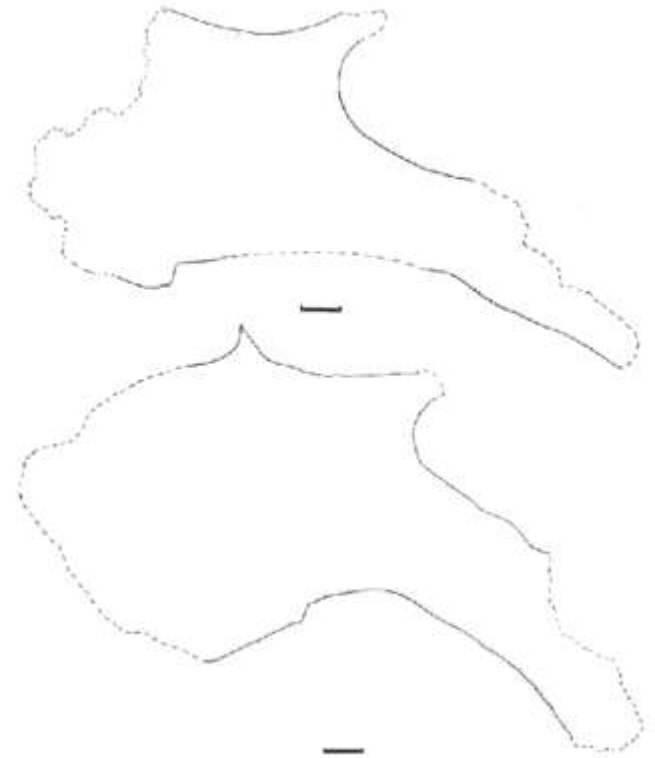

FIGURE 15—*S. ferocior*. Outline of jugals (UCMP 34196 and 83208) showing different degrees of downturning of the posterior process. Scale equals 1 cm.

element is essentially a triangular sheet of thin bone. It is lightly sculptured and does not display sutural surfaces to any great extent. A narrow ridge extends for 4-8 mm posteroventrad from the posterior surface of the element. This ridge marks the apparent origin of the depressor mandibulae. Above this ridge the squamosal becomes narrow and the sutural surface for the postorbital becomes just visible.

In posterior view (Fig. 16B) sutural surfaces lateral and medial to the point of origin of the depressor mandibulae mark the extent of the supratemporal and tabular contacts, respectively. Below the ridge, however, the posterior surface is smooth. A slight, laterally placed and vertically oriented ridge marks the lateral extent of the depressor mandibulae and other musculature tissue. At midheight, along the medial edge of the posterior surface, a slight thickening and a heavily scarred area mark the point of contact with the tip of the paroccipital process. Above this area the posterior surface expands mediad as a thin sheet of bone. This is somewhat depressed forward and contains a small pit in the center, the function of which is unknown.

The supraoccipital may have gained contact with the medial extent of this lamina, but no evidence for this is demonstrable. The tabular appears to have overlain this extensive region of the squamosal as it extended dorsolaterad to the medial edge of the groove marking the contact of the postorbital. No evidence for a contact between the squamosal and parietal is present in any of the specimens.

In anterior view (Fig. 16C) sutural scars mark the contacts of the quadratojugal in the ventrolateral corner, and the quadrate medial to this. Barely visible in this view is the sutural surface for the jugal. The border of the temporal fenestra is somewhat thickened and light striae radiate from it anteroventrad. At the posteroventral corner of the temporal fenestra there is a slight horizontal ridge of unknown function.

Tabular (1 specimen)

The tabular (Fig. 17) forms the lateral—dorsolateral edge of the occiput and is a fairly massive element. In occipital view the left tabular appears as an upsidedown L. The dorsal and lateral edges of the element form a continuous, upraised ridge that forms the boundary between the occiput, and the skull table and cheek. The posteroventral edge of the parietal is wedged into a groove that lies along the dorsal edge of the tabular. This wedge-like contact may prevent contact between the squamosal and the parietal. Along the dorsal edge of the tabular, where the tabular approaches the midline, a more gentle overlapping contact of the tabular on the parietal results in the loss of the ridge previously mentioned. The tabular is probably overlain by the postparietal close to the mid-line.

The supraoccipital is also wedged into the ventral and medial edges of the tabular. Fig. 17 shows a cross-sectional break through the tabular. Ventrolateral to this cross section the tabular turns ventrad and forms the lateral border of the post-temporal fenestra. Beyond the fenestra, the extent of the tabular can only

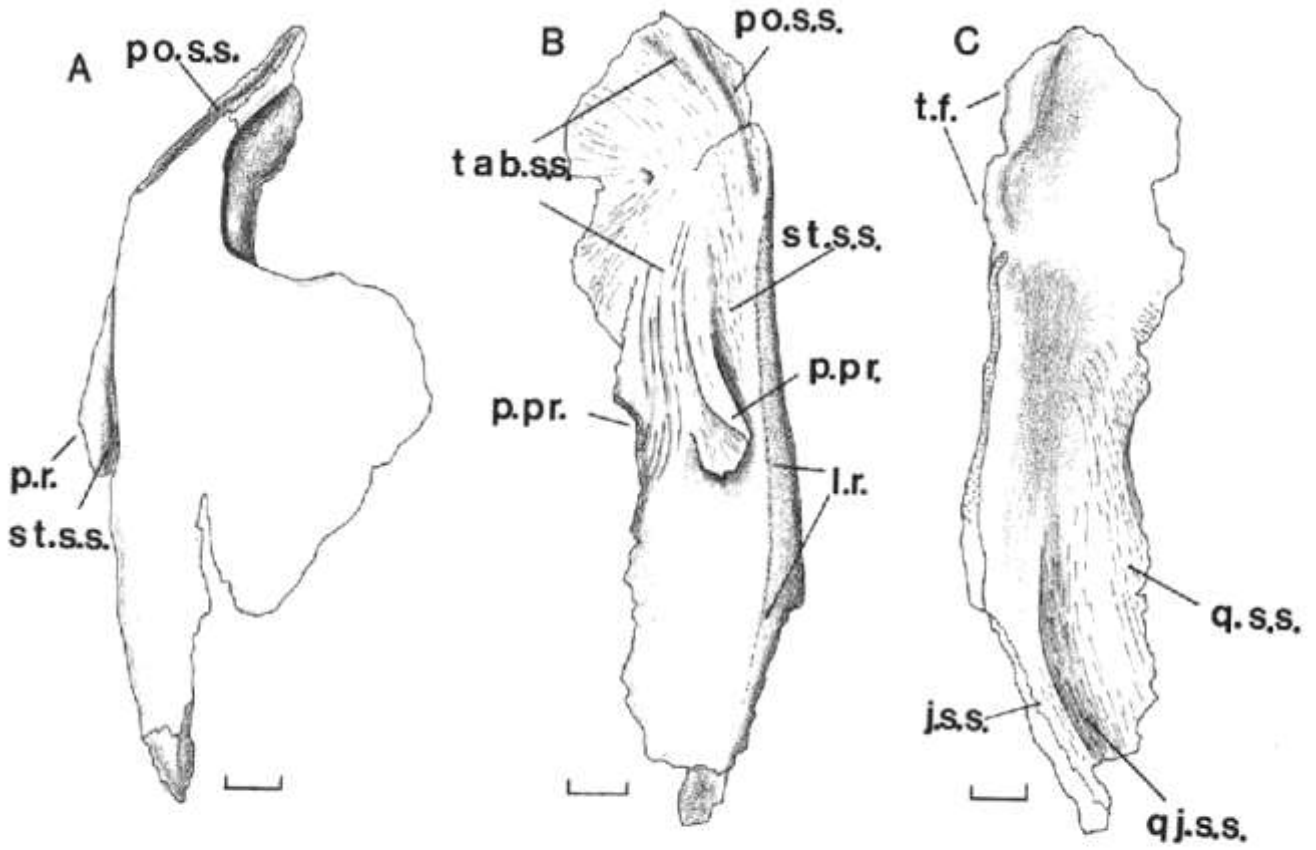

FIGURE 16—*S. ferocior.* Right squamosal (UCMP 34196): **A,** lateral view; **B,** posterior view; **C,** anterior view. Abbreviations: **j.s.s.,** jugal sutural surface; **l.r.,** lateral ridge; **p.r.,** posterior ridge; **p.pr.,** paroccipital-process contact; **po.s.s.,** postorbital sutural surface; **q.s.s.,** sutural surface for quadrate; **qj.s.s.,** quadratojugal sutural surface; **st.s.s.,** supratemporal sutural surface; **t.f.,** border of temporal fenestra; **tab.s.s.,** sutural surface for tabular. Scale equals 1 cm.

be inferred from the squamosal, and is discussed **with that element.**

Supratemporal (no specimens)

No isolated supratemporals exist in the collections of *S. ferocior* **from the Anderson quarry. However, the size and extent of the element can be largely deduced from the presence of its sutural scars on adjacent elements as well as by examining its presence in one highly distorted skull of** *S. ferox* **(U.C. 35). Fig. 18 is an outline drawing of U.C. 35 in occipital view. On either side the narrow supratemporal contacts the squamosal medial to, and above the level of, the process for the adductor mandibulae. The element continues dorsad to overlie the external surface of the parietal wing. However, the extent of its contact with the postorbital is unknown.**

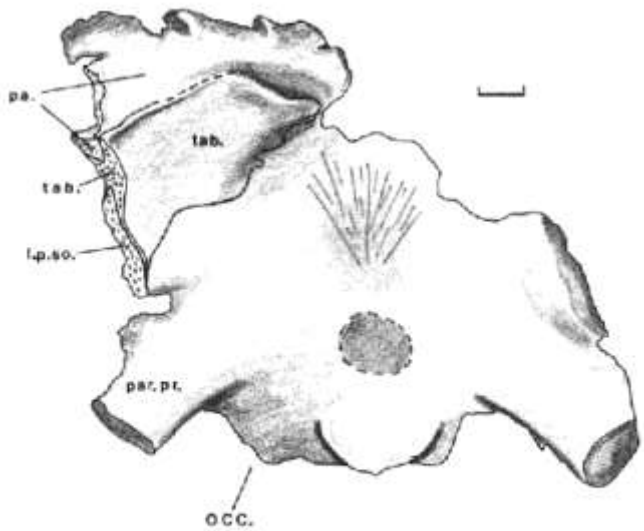

FIGURE 17—*S. ferocior.* Left tabular (MCZ 1489). Abbreviations: **Occ.,** occiput; **l.p.so.,** lateral process of supraoccipital; **pa.,** parietal; **par.pr.,** paroccipital process; **tab.,** tabular. Scale equals 1 cm.

Vomer (2 specimens)

Paired vomers in *5. ferocior* **are** known only in the type (MCZ 1489) and are poorly preserved. The right vomer (Fig. 19A, B) retains its anterior contact **with the premaxilla, but has lost much of the dorsal lamina. Conversely, the left vomer (Fig. 19C) has been displaced dorsad and contact with *the* premaxilla, pterygoid, and palatine has been lost, but much of the dorsal lamina is still present.**

The posterior end of the element is U-shaped in cross section (Fig. 19A) and is overlain by the pterygoid medially and the palatine laterally. The dorsal lamina of the vomer is continuous with the dorsal lamina of the pterygoid and serves as the medial limit of the nasal capsule. Still in lateral view (Fig. **19A), and beginning at a position just posterior to the mid-**

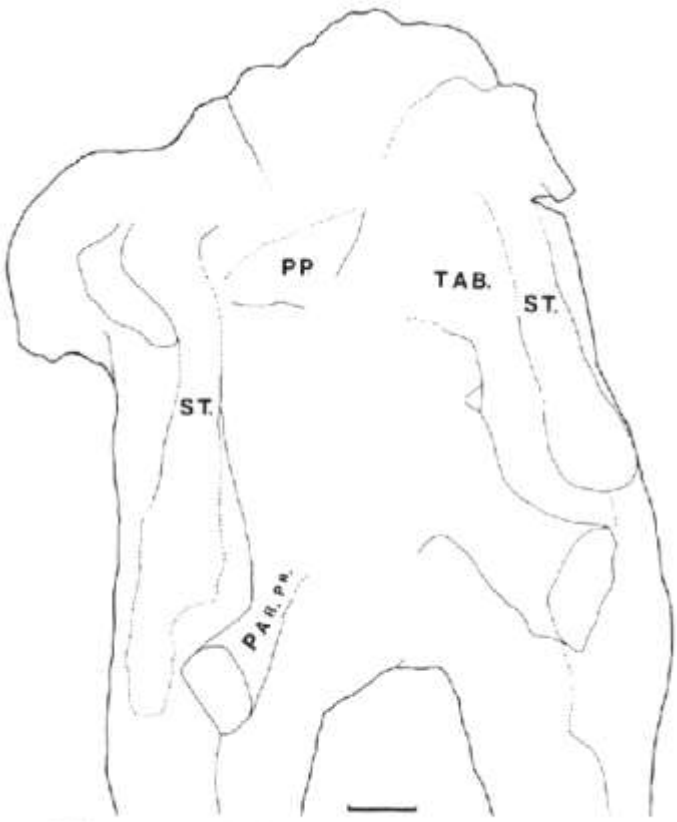

FIGURE 18—*S. ferox*. Right and left supratemporals (U.C. 35). Abbreviations: **pp.**, postparietal; **par.pr.**, paroccipital process; **st.**, supratemporal; **tab.**, tabular. Scale equals 1 cm.

length of the element, a narrow groove runs forward to the anterior border of the element where it deepens and receives the narrow vomerine process of the pre-maxilla.

Fig. 19B shows the right vomer in medial view. The dorsomedial surface contacts the opposing vomer. Above this area of contact, an anteroposteriorly elongate groove offsets the remainder of the dorsal lamina laterad, thus preventing further contact between the medial surfaces of the vomers.

In dorsal or ventral view (Fig. 20B, C) the palatine is subtriangular and forms the anterolateral floor of the palate. UCMP 83285 (Fig. 20) only lacks the delicate posterior and medial edges.

Fig. 20A shows the palatine in lateral view. The lateral edge is thick and forms a shelf that contacts the medial and dorsal surfaces of the alveolar ridge of the maxilla well posterior to the caniniform buttress. Contact between the palatine and the alveolar ridge just behind the caniniform buttress appears to have been of an abutting type, not involving an overlapping shelf.

Above the maxillary contact the anterolateral surface of the palatine is extensively marked with vessel scars, some of which can be matched with those on the maxilla. The maxillary and possibly the lateral palatine arteries run along the dorsolateral surface of the palatine (Fig. 20B). At about midlength, a branch runs onto the dorsal surface of the alveolar ridge of the maxilla as described for that element. The remaining branch on the palatine runs onto the lateral surface of the palatine and then continues forward, bifurcating as shown in Fig. 20A. The vomerine process of the palatine extends anterodorsad and is separated from the maxillary process of the palatine by the narrow, posterior extension of the internal flares.

In ventral view (Fig. 20C) a small, scarred region along the anteromedial surface of the palatine represents the area of contact with the pterygoid. In dorsal view (Fig. 20B) the pterygoid contact on the maxillary process is just visible. Posterior to this, along the dorsal inner edge of the medial wall, is a narrow sutural scar. It is tentatively interpreted as a scar marking the contact between the palatine and the pterygoid. The actual manner in which the vomer, pterygoid, and palatine come together is difficult to determine on the basis of disarticulated material.

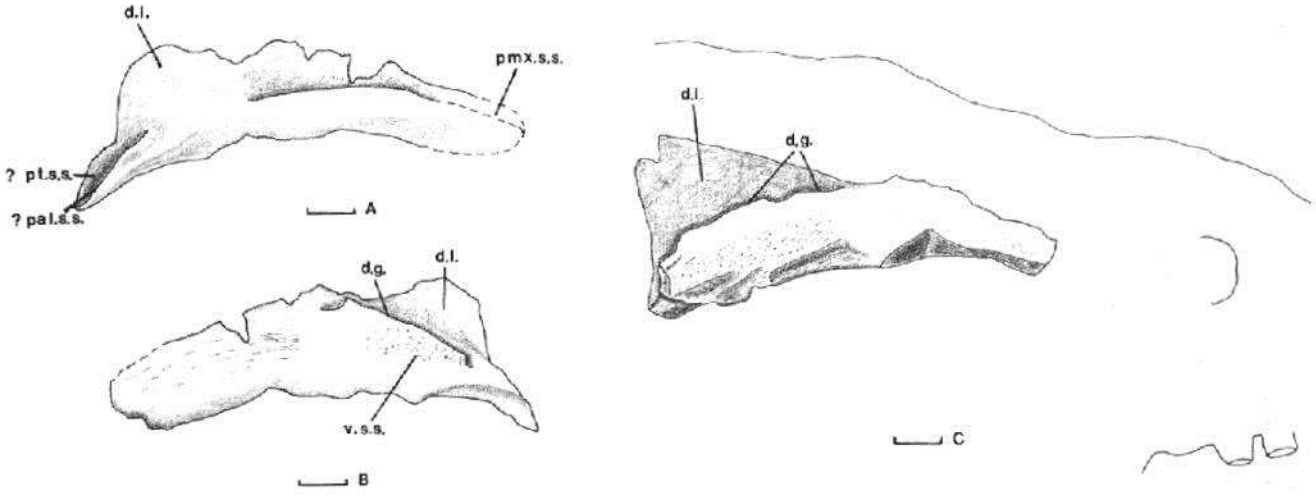

FIGURE 19—*S. ferocior*. Right and left vomers (MCZ 1489): **A**, right vomer, lateral view; **B**, right vomer, medial view; **C**, left vomer, medial view. Abbreviations: **d.g.**, dorsal groove; **d.l.**, dorsal lamina; **pal.s.s.**, sutural surface for palatine; **pmx.s.s.**, premaxillary sutural surface; **pt.s.s.**, pterygoidal sutural surface; **v.s.s.**, sutural surface for vomer. Scale equals 1 cm.

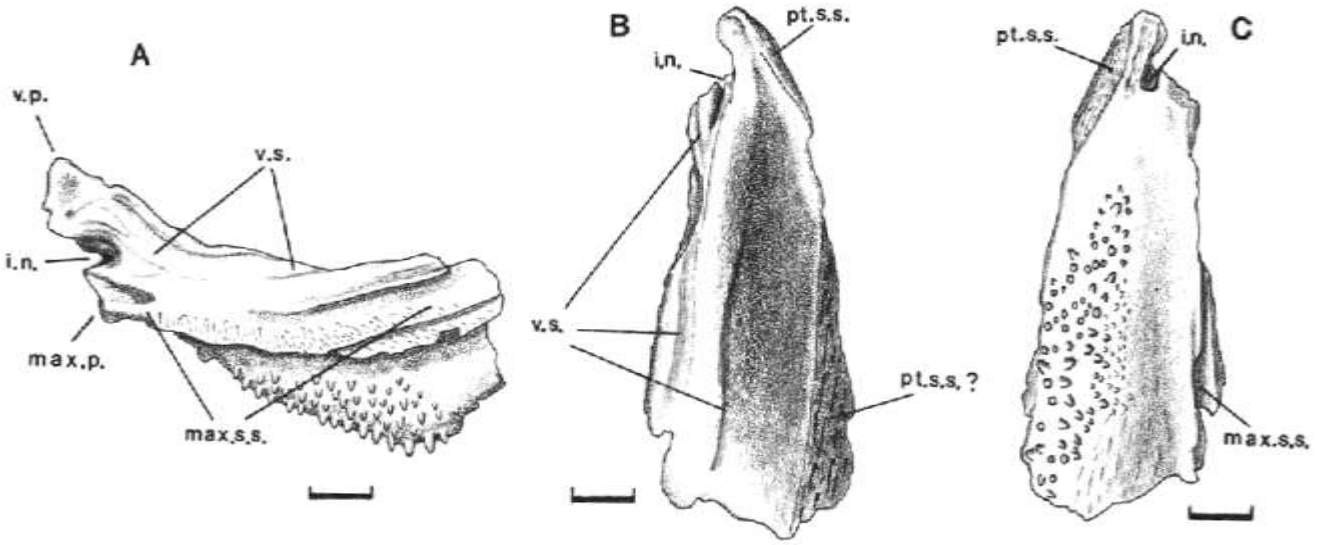

FIGURE 20—*S. ferocior*. Left palatine (UCMP 83285): **A**, lateral view; **B**, dorsal view; **C**, ventral view. Abbreviations: **i.n.**, internal nares; **max.p.**, maxillary process; **max.s.s.**, maxillary sutural surface; **pt.s.s.**, pterygoidal sutural surface; **v.p.**, vomerine process; **v.s.**, vessel scar. Scale equals 1 cm.

The ventral surface of the palatine is a thin sheet that is toothed and strongly convex ventrad. The tooth field appears to be well developed in the figured specimen and the teeth are largest at the deepest extent of the element. The nature of the contact with the ectopterygoid is unclear. The posterior edge of the ventral surface of the palatine is lightly scarred and might mark an area where the ectopterygoid comes into contact with the element.

Ectopterygoid (no specimens)

There are no clear examples of ectopterygoids in the UCMP *Sphenacodon* collection or in collections of *Sphenacodon* in other museums. The element occurs in *Dimetrodon* anterolateral to the transverse flange of the pterygoid, posterior to the palatine, and medial to the jugal (Romer and Price, 1940; Reisz, 1980). Among these elements in the UCMP *Sphenacodon* collection, only the palatine shows sutural scars that have been tentatively identified as those resulting from a contact with the ectopterygoid (Fig. 20C). The description of the ectopterygoid will have to await better preserved material.

Pterygoid (35 specimens)

Fig. 21A shows the pterygoid in medial view. The large vertical, dorsal lamina of the palatal process is separated from the ventrally convex, toothed palatal surface by an elongate ridge which also marks the line of contact between the paired pterygoids. The dorsal lamina is continuous with the dorsal lamina of the vomer and, as in the latter element, serves as the medial wall of the nasal capsule. The edges of the palatal process are missing and sutural scars thus are largely absent. It is thought, however, that the pterygoid contacts the medial—ventromedial surface of the vomerine process of the palatine; together the pterygoid and palatine are underlain by the posterior end of the vomer.

Still in medial view, the transverse flange of the pterygoid dips laterad; six prominent teeth point mediad and slightly forward. The jugal process extends dorsolaterad from the transverse flange to make contact with the jugal. Along the dorsal edge of the quadrate process of the pterygoid, just posterior to the transverse flange, a deep groove marks the area where the epipterygoid contacts the pterygoid.

The full extent of the palatal-tooth field is visible in ventral view (Fig. 21B). Teeth are arranged randomly in this field. Anterolateral to the tooth field, a series of grooves and ridges marks the area of contact with the posteromedial surface of the palatine.

A small portion of the palatal-tooth field, the sutural surface for the jugal, and the incised area for the epipterygoid contact are all visible in lateral view (Fig. 21C). At the posterior end of the quadrate process, a series of extensive scars marks the extent of the pterygoid's contact with the quadrate.

Epipterygoid (3 specimens)

The three known epipterygoids are poorly preserved, lacking much of the extremities. Fig. 22A shows a right epipterygoid in medial view. The anterior border of the bone is thickened and circular in cross section. The dorsal apex of the anterior border ends in unfinished bone. Behind the thick, rounded border, the remainder of the element becomes a flattened sheet of bone. The articular area for the basipterygoid processes is roughly oval in medial view and possesses two facets whose surfaces are unfinished. The more dorsal of the two faces anteroventromediad at about 30° from the vertical. The smaller ventral facet faces anterodorsomediad. These orientations are difficult to justify in light of the corresponding orientations of basipterygoid processes. This probably reflects a certain degree of overpreparation and the undoubted presence of a cartilaginous region between the two. However, there is no doubt that two distinct facets

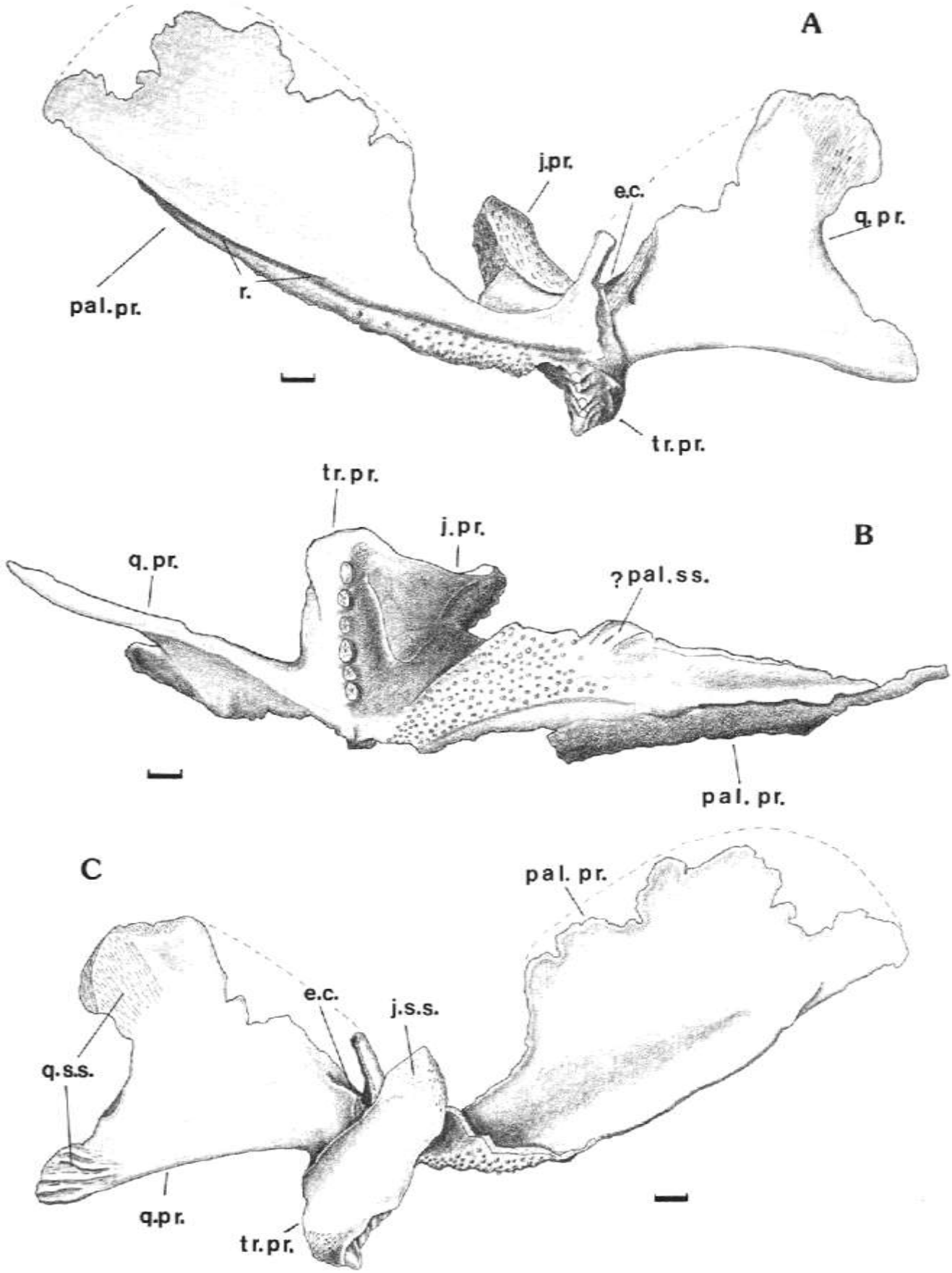

FIGURE 21—*S. ferocior*. Right pterygoid (MCZ 1489): **A**, medial view; **B**, ventral view; **C**, lateral view. Abbreviations: **e.c.**, epipterygoidal contact; **j.pr.**, jugal process; **j.s.s.**, jugal sutural surface; **pal.pr.**, palatal process; **pal.s.s.**, sutural surface for palatine; **q.pr.**, quadrate process; **q.s.s.**, sutural surface for quadrate; **r.**, ridge; **tr.pr.**, transverse flange. Scale equals 1 cm.

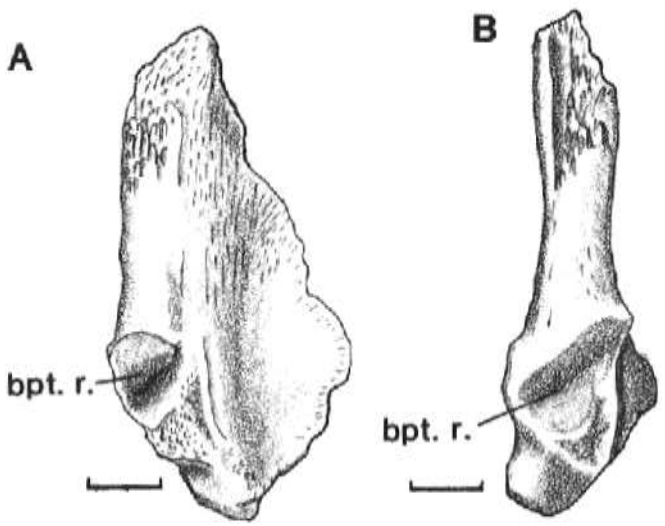

FIGURE 22—*S. ferocior.* Right epipterygoid (MCZ 1489): **A,** medial view; **B,** anterior view. Abbreviation: **bpt.r.,** recess for basipterygoid process. Scale equals 1 cm.

are present. Ventral to the facets the bone becomes thinner, still retaining a rounded anterior surface. The ventral edge of the element is incomplete and the edges that contact both the quadrate ramus of the pterygoid and the dorsal tip of the quadrate are not preserved.

Quadrate—quadratojugal (27 specimens)

In lateral view (Fig. 23C) the quadrate is a relatively large, flattened, diamond-shaped bone. It has two anteroposteriorly elongate condyles ventrally that contact the articular of the mandible, and a slight sutural scar along its posterolateral edge marking the contact with the squamosal. In medial view (Fig. 23D) the sutural surface for the pterygoid begins as a V-shaped indentation above the medial condyle. This sutural surface continues along the leading edge to within **1** cm of the apex of the quadrate where a difference in scarring and a slight ridge mark the pterygoid's dorsal limit. The extent of the contact with the epipterygoid is not readily apparent. The ventral half of the pterygoid contact area is rugose, deeply scarred, and is bordered anteriorly and posteriorly by slightly thickened ridges. The dorsal half of the pterygoid contact area is only lightly scarred. Just posterior to this dorsal limit of the pterygoid, a region of light scarring extends ventrad a short distance from the apex of the quadrate. This scar marks the extent of the quadrate's contact with the paroccipital process.

Above the medial condyle and adjacent to the pterygoid sutural surface a shallow excavation receives the cartilaginous extension of the ventral process of the stapes.

In ventral view (Fig. 23B) the anteroposteriorly elongate axes of the condyles converge slightly in front of the condyles. The medial condyle is positioned slightly ahead of, and lower than, the lateral condyle.

The posterior border of the quadrate (Fig. 23D) bears the sutural scars for the squamosal and the quadratojugal. This single sutural surface extends from about

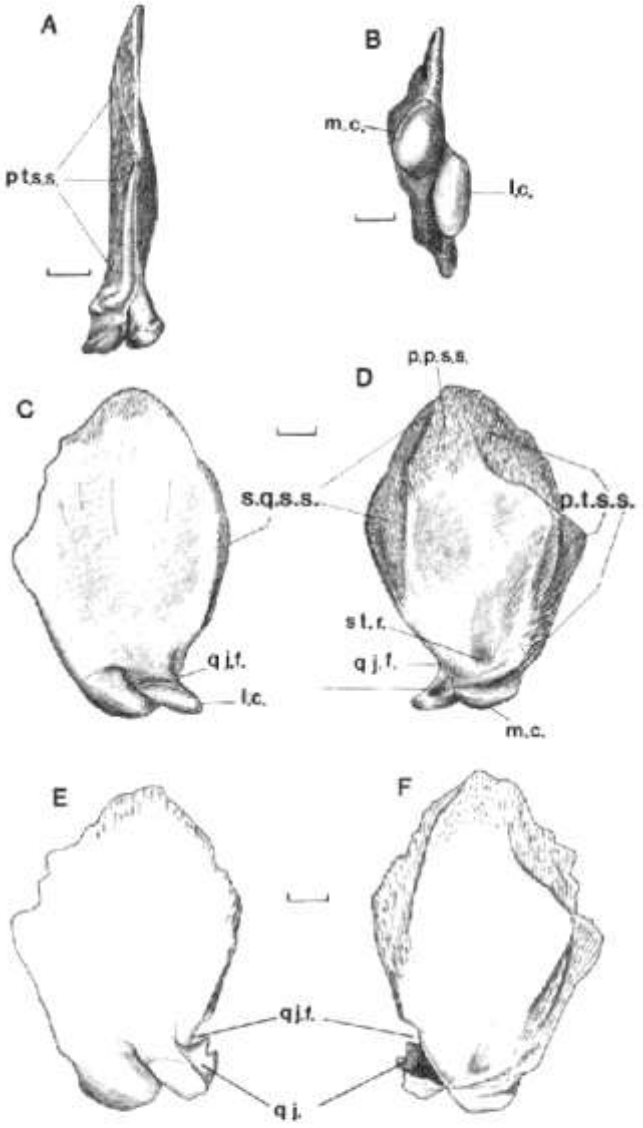

FIGURE 23—*S. ferocior.* Left quadrate and quadratojugal (UCMP 34219): **A,** anterior view; **B,** ventral view; **C** and **E,** lateral views; **D** and **F,** medial views. Abbreviations: **l.c.,** lateral condyle; **m.c.,** medial condyle; **p.p.s.s.,** sutural surface for paroccipital process; **pt.s.s.,** pterygoidal sutural surface; **qj.,** quadratojugal; **qj.f.,** quadratojugal foramen; **s.q.s.s.,** squamosal–quadratojugal sutural surface; **st.r.,** stapedial recess. Scale equals 1 cm.

2 cm above the ventral surface of the lateral condyle to just below the dorsal apex of the quadrate. Although complete quadratojugals are unknown, this sutural surface suggests that the quadratojugal was a tall, narrow element. Fig. 23C, D shows the ventral portion of the quadratojugal sutured to the dorsal surface of the lateral condyle. A region of unscarred bone above this seat marks the probable position of the quadratojugal foramen.

Basioccipital (8 specimens)

The basioccipital is fairly well represented in the Anderson quarry collection and is most commonly found with articulated braincases. In all specimens the element is convex ventrally (posterior view, Fig. 24A), forms the ventral portion of the occipital con-

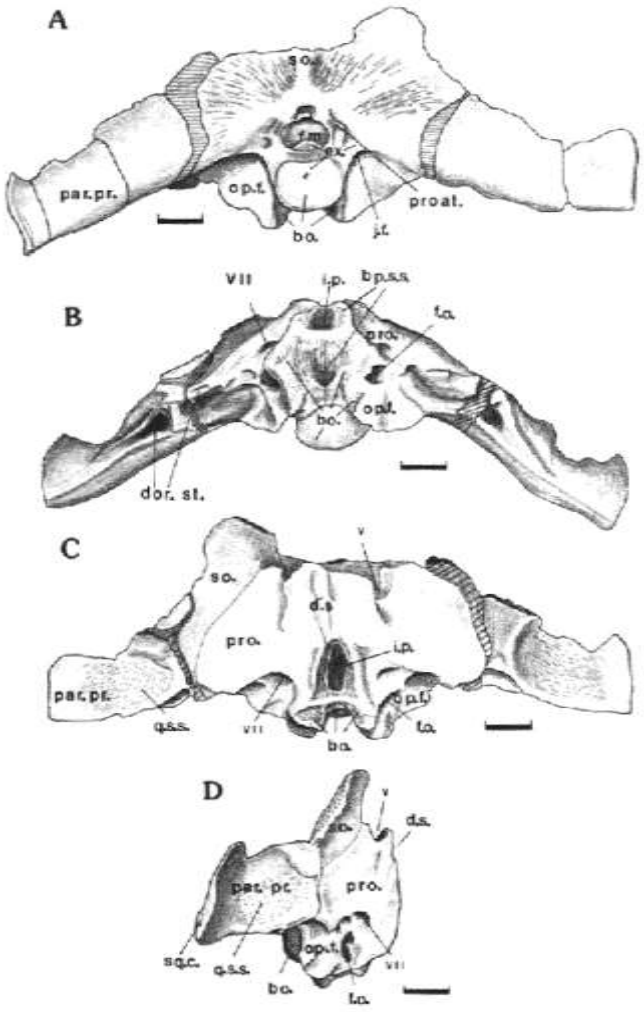

FIGURE 24—*S. ferocior*. Occiput and braincase (UCMP 34218): **A,** occipital view; **B,** ventral view; **C,** anterior view; **D,** lateral view. Abbreviations: **bo.**, basioccipital; **bp.s.s.**, sutural surface for basipterygoid; **d.s.**, dorsum sellae; **dor.st.**, dorsal head of stapes contact; **ex.**, exoccipital; **f.m.**, foramen magnum; **f.o.**, fenestra ovalis; **i.p.**, position of infundibulum; **j.f.**, jugular foramen; **op.f.**, flange of opisthotic; **par.pr.**, paroccipital process; **pro.**, prootic; **proat.**, proatlas contact; **q.s.s.**, sutural surface for quadrate; **sq.c.**, squamosal contact; **so.**, supraoccipital; **V**, trigeminal foramen; **VII**, foramen for seventh cranial nerve. Scale equals 1 cm.

dyle, and is indistinguishably fused with the exoccipitals. Laterally positioned, ventrad projecting processes of the basioccipital each brace the adjacent opisthotic in the region posterior to the fenestra ovalis. The processes also run forward along the ventral surface of the braincase (Fig. 24B) and are separated from one another by the concave, scarred, ventral surface of the basioccipital. The medial surface of the process shows scarring where it becomes applied against the medial, inner surface of the basiparasphenoid tubera. A bar of bone, perhaps composed of exoccipital as well as basioccipital, separates the anterior infundibular region from this posterior basiparasphenoidal sutural surface.

Exoccipital (5 specimens)

Exoccipitals are known from five articulated braincases. The exoccipitals (Fig. 24A) form the lateral walls of the foramen magnum and are excluded from contact with one another dorsally by a small portion of the supraoccipital. They are indistinct from the adjacent opisthotics, but can be identified by the facets for the proatlas contact. Ventral to these facets each extends laterad as a small wedge beneath the ventral border of the paroccipital process.

The exoccipitals are also indistinguishably fused with the basioccipital, but the notochordal pit probably marks the ventral extent of the exoccipitals. Viewed through the foramen magnum, the exoccipitals meet in the midline to form the floor of the braincase in this region. A slight ridge along the midline marks their mutual contact.

Supraoccipital (10 specimens)

The supraoccipital forms most of the large occipital plate. Its limits are difficult to delineate, however, because of the fusion that occurs between braincase elements in larger specimens. Fig. 25A shows the supraoccipital in posterior view. A massive and broad dorsal process rises above the body of the element and terminates in a thick, unfinished surface. Apparently a cartilaginous forward extension from this surface forms the roof of the braincase in the region beneath the parietal. The posterior surface of the **dorsal** process is deeply scarred, marking the extent of the postparietal's contact in the midline and the tab-

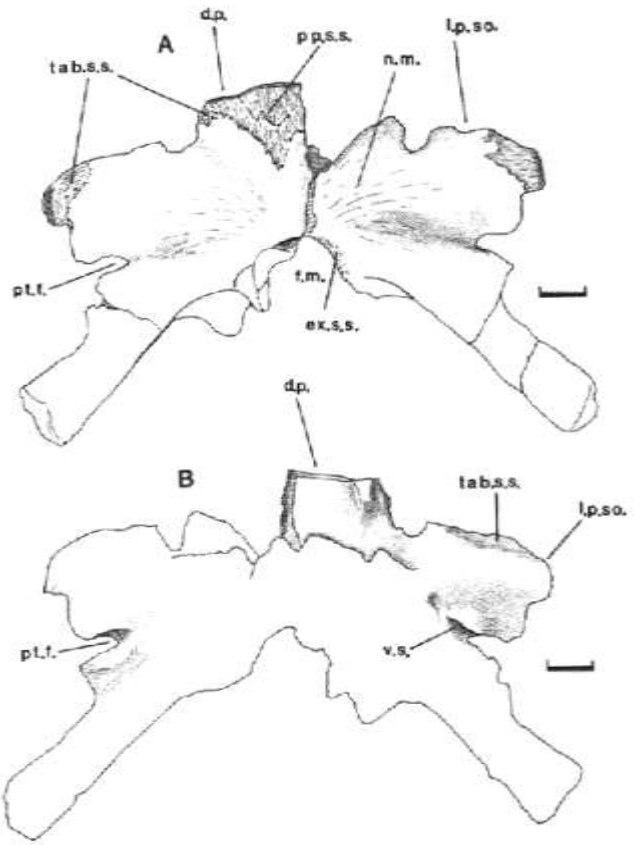

FIGURE 25—*S. ferocior*. Supraoccipital (UCMP 83251): **A,** posterior view; **B,** anterior view. Abbreviations: **d.p.**, dorsal process; **ex.s.s.**, exoccipital sutural surface; **f.m.**, foramen magnum; **l.p.so.**, lateral process of supraoccipital; **n.m.**, neck muscle scars; **pp.s.s.**, postparietal sutural surface; **pt.f.**, post-temporal foramen; **tab.s.s.**, sutural surface for tabular. Scale equals 1 cm.

ular's contact at the dorsolateral corner. Paired lateral processes extend horizontally almost as far as the tip of the paroccipital process. They become thin along their ventral edge. The tip of each process is thickened and heavily scarred, marking the extent of the tabular's contact. A gap between each lateral process and paroccipital process marks the position of the small post-temporal fenestrae and probably represents the ventral extent of the supraoccipital medial to it. A thickened vertical ridge occurs in the midline of the supraoccipital. A series of light striae, marking the insertional area for neck musculature, radiates from it. Below the ridge, the supraoccipital is narrowly exposed in the foramen magnum.

In anterior view (Fig. 25B) the surface of the dorsal process is smooth and is notable only for the presence of paired blunt processes projecting forward from the dorsolateral corners (only one is visible in Fig. 25B). A light sutural scar for the tabular is visible along the dorsal edge of the lateral process. A vascular groove runs a short distance mediad from the medial edge of the post-temporal fenestra.

Opisthotic (10 specimens)

The opisthotic forms the ventrolateral portion of the braincase, including the elongate paroccipital process and the lateral walls of the otic capsule posterior to the fenestra ovalis. In posterior view (Fig. 24A) the paroccipital processes run from the position of the foramen magnum posteroventrolaterad to contact the squamosal. The distal ends of the processes become compressed anteroposteriorly, ending in unfinished bone that is somewhat visible in posterior view. Adjacent to the basioccipital, each opisthotic forms a thin, fan-shaped flange that fills the space between the ventral edge of the paroccipital process and the ventrad projecting basioccipital process. The jugular foramen occurs at the juncture between the exoccipital and the opisthotic flange, just above the level of the occipital condyle.

Figs. 24A and 25A show occipital views of two braincases from the Anderson quarry. A certain amount of variation in the orientation of the paroccipital processes is noticeable. Fig. 25A shows the processes projecting posteroventrolaterad at about 40° below the horizontal. Fig. 24A shows the paroccipital processes directed posteroventrolaterad at about 20° below the horizontal. This situation is reminiscent of the variation displayed in the jugals (Fig. 15), and was taken into account in the two reconstructions (Fig. 3A, B).

In ventral view (Fig. 24B), lateral to the ventral flanges of the opisthotics, the paroccipital processes are excavated to receive the broad dorsal head of the stapes. Much of this area is distorted by breakage, however, and details are unclear.

In lateral view (Fig. 24D) the fenestra ovalis appears as an oval opening in the ventrolateral plane. In this region as well, distortion makes interpretation of the details unreliable.

Prootic (10 specimens)

The remainder of the otic region of the braincase consists of large paired prootics that fuse to form the prootic bridge or dorsum sellae anterior and medial to the notch for the trigeminal nerve. In lateral view (Fig. 24D) the prootic fuses with the opisthotic along a line that runs from the level of the post-temporal fenestra to the anteroventral edge of the paroccipital process and then ventromediad, above and then in front of the fenestra ovalis. It is 'assumed that the lateral surface of the otic capsule, anterior to the fenestra ovalis, consists solely of prootic and that the edges of the opening for the infundibulum are the surfaces where the prootic contacts the basisphenoid (Romer and Price, 1940, pp. 41-72).

Dorsal to the infundibular pit (Fig. 24C) the prootics fuse in the midline to form the dorsum sellae. A slight ridge visible in the midline marks the line of fusion. The dorsolateral edge of the dorsum sellae is notched, marking the point of exit of the trigeminal nerve. The prootic is distinguished from the supraoccipital by a slight groove that extends ventrad from just posterior to the notch for the trigeminal nerve.

The foramen for the VIIth cranial nerve can be seen dorsal and slightly anterior to the fenestra ovalis in ventral, anterior, and medial views. A shallow depression of unknown function appears slightly lateral and ventral to the foramen.

Basiparasphenoid (3 specimens)

Although the basisphenoid and parasphenoid are separate elements, their fusion early in ontogeny justifies discussing their morphology in the same section. The ventral surface of the basiparasphenoid consists primarily of the parasphenoid. The dorsal and internal surfaces are formed by the basisphenoid. The tubera form the widest portion of the complex and appear as two separate projections, convex ventrad (Fig. 26B) and concave dorsad (Fig. 26C). In lateral view (Fig. 26C) the tubera are open posteriorly and the internal surface consists of unfinished bone. The dorsal surfaces of the lateral edges of the tubera contact the ridges formed by the basioccipital and prootic contact, medial to the foramen for the VIIth cranial nerve. The tubera extend just posterior to the position of the fenestra ovalis and may contact the footplate of the stapes. The posterior edges of the tubera (Fig. 26B, C) appear thickened and heavily marked by striae. Romer and Price (1940) hypothesized that these striae in *Dimetrodon* result from the insertion of the prevertebral musculature.

In ventral view (Fig. 26B) the tubera converge anteriorly and a narrow shelf forms between them. Anterior to this shelf are the two anterolaterad projecting basipterygoid processes. The processes display two distinct facets: a lower facet that faces anteroventrolaterad and an upper facet that faces anterodorsolaterad. A foramen for the carotid artery is present posterior to the neck of each basipterygoid process (Fig. 26B).

In lateral view (Fig. 26A, C) the basiparasphenoid has a pair of posteriorly concave pillars positioned slightly behind a vertical line drawn through the basipterygoid processes. The inner surfaces of the pillars contact the inner and outer edges of the infundibular

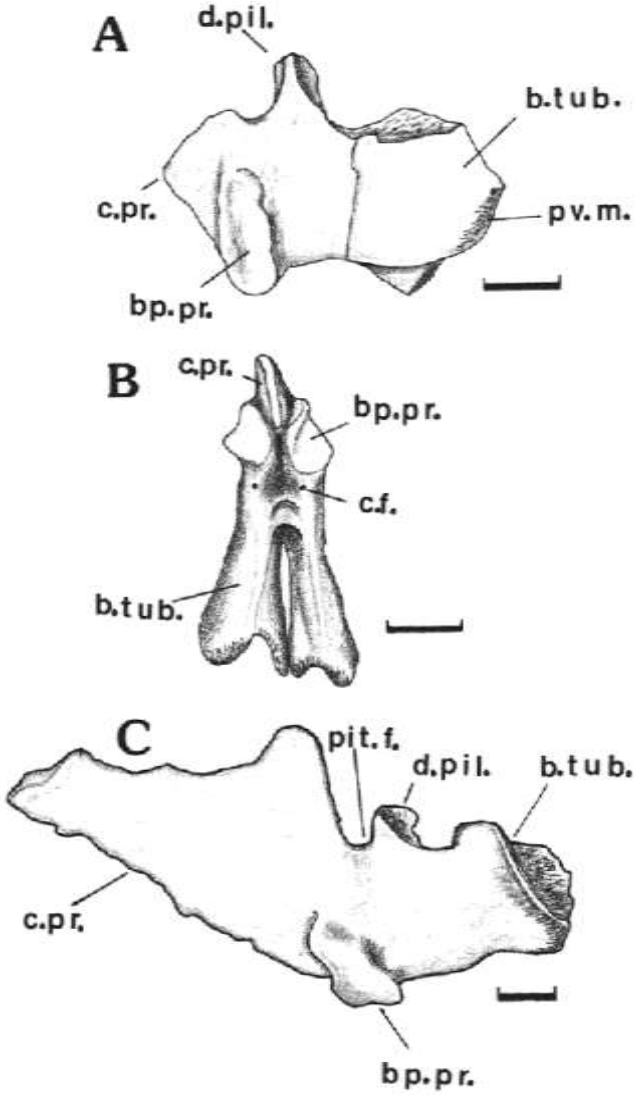

FIGURE 26—*S. ferocior*. Basiparasphenoid: **A**, lateral view (UCMP 34218); **B**, ventral view (UCMP 34218); **C**, lateral view (MCZ 1489). Abbreviations: **b.tub.**, basal tubera; **bp.pr.**, basipterygoid process; **c.f.**, carotid foramen; **c.pr.**, cultriform process; **d.pil.**, dorsal pillae; **pit.f.**, pituitary fossa; **pv.m.**, prevertebral muscle scars. Scale equals 1 cm.

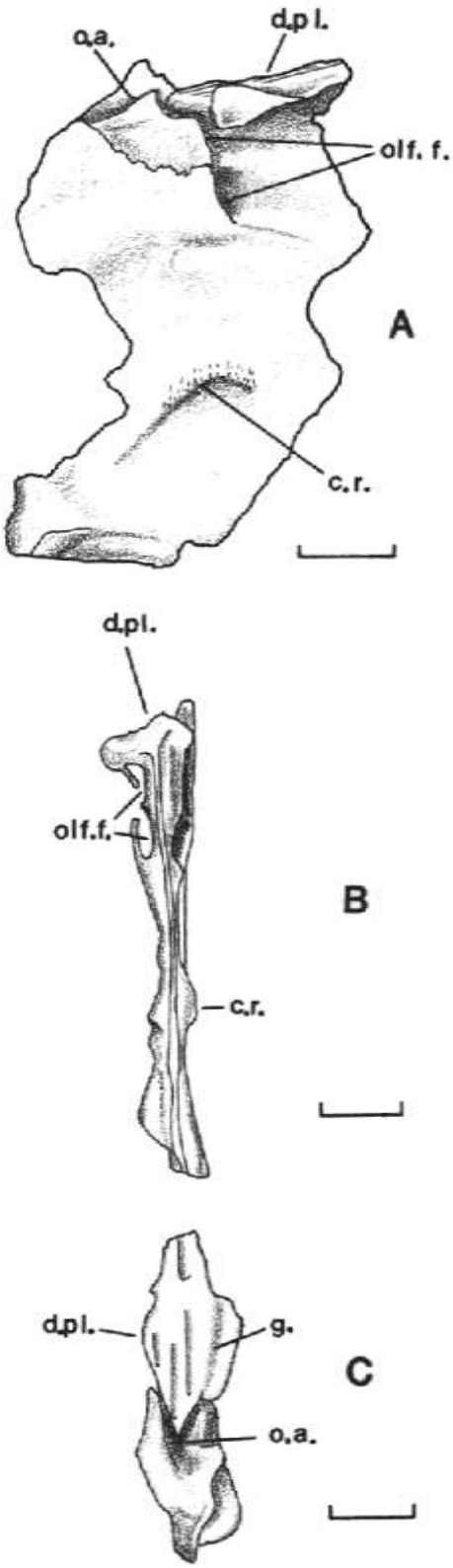

FIGURE 27—*S. ferocior*. Sphenethmoid (UCMP 34218): **A**, lateral view; **B**, anterior view; **C**, dorsal view. Abbreviations: **c.r.**, ridge; **d.pl.**, dorsal plate; **g.**, groove; **o.a.**, open area posterior to plate; **olf.f.**, olfactory foramen. Scale equals 1 cm.

pit. In the midline, anterior to the pillars, the pituitary fossa marks the position of the pituitary.

Anterior to the pituitary fossa the cultriform process arches dorsad and continues forward to contact the sphenethmoid. The process is V-shaped in cross section and is made up of very thin bone that is apparently highly susceptible to distortion.

Sphenethmoid (1 specimen)

The sphenethmoid is a thin plate of bone that rests within the cultriform process and extends dorsad to the skull roof. The bone is dorsally hollow and is covered by a diamond-shaped plate of unfinished bone (Fig. 27C). The surface of the plate is lightly marked with anteroposteriorly oriented striae and paired grooves run from the anterolateral corners to the posterior apex.

In lateral and anterior views (Fig. 27A, B, respec**tively) two foramina are visible on either side, opening anteriorly just below the dorsal surface of the element on the midlateral surface. The foramina appear to have been involved in transmitting the paired**

olfactory nerves forward to the snout. The entry point of the olfactory tract was probably a single foramen in the posterior surface of the element. The posterior surface is poorly preserved, however, and details in this region are unclear.

A small crescentic ridge, concave ventrad, is visible on the lateral surfaces (Fig. 27A). This ridge marks the contact of the medial surface of the cultriform process with the sphenethmoid. The sphenethmoid is poorly preserved ventrally, but enough remains to demonstrate a slight amount of thickening in the region where the sphenethmoid rests in the cultriform process.

Stapes (4 specimens)

The stapes consists of an anteroposteriorly flattened plate and an ovate, dorsomediad projecting, concave footplate that articulates with the fenestra ovalis.

Most of the important morphological features are visible in posterior view (Fig. 28A). The body of the element is thickened along the medial edge beneath the footplate, tapers slightly as it extends ventrolaterad, and ends as an unfinished blunt process. A slight ridge of unknown function lies parallel to the medial edge. The dorsal process lies lateral to the footplate and is separated from it by a shallow notch. The dorsal process thickens and widens slightly as it extends dorsad above the level of the footplate. Its dorsal edge is unfinished and makes contact with the groove in the ventral surface of the paroccipital process.

The neck separating the body of the stapes from the footplate is narrow and perforated by a large stapedial foramen which measures 4-4.5 mm in diameter. A slim bar of bone that formed the dorsal border of the foramen has been lost in all of the available specimens.

The footplate is oval in medial view (Fig. 28B) and its medial surface is unfinished. The exact contours of the surface are thus unclear.

In anterior view (Fig. 28C) the medial edge of the body of the element is shallowly excavated. Romer and Price (1940, p. 88) suggest that a similar excavation **in** *Dimetrodon* results from a ligamentous attachment between the stapes and the stapedial pit of the quadrate.

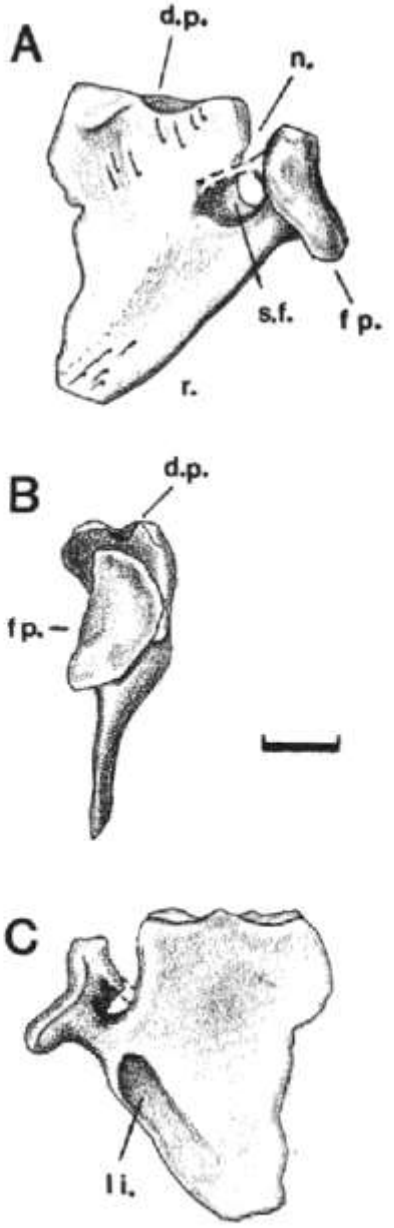

FIGURE 28—*S. ferocior.* Reconstruction of left stapes based upon UCMP 123288 and 125583: **A**, posterior view; **B**, medial view; **C**, anterior view. Abbreviations: **d.pr.**, dorsal process; **fp.**, footplate; **li.**, ligamentous contact?; **r.**, ridge; **st.f.**, stapedial foramen. Scale equals 1 cm.

Lower jaw

Dentary (32 specimens)

The dentary is the tooth-bearing element of the mandible and is the most massive element in the lower jaw, extending three-quarters of its total length. Of the 32 dentaries and dentary fragments present in the UCMP collection, 14 show complete dental counts. These range from 20 to 26 (Table 2). No juvenile lower jaws are present in the collection and subadult dentaries are difficult to distinguish from adult dentaries. Thus, ontogenetically controlled tooth-count variation is not understood in this sample. In all the dentaries examined there is only one moderately sized precaniniform tooth followed by space for two large caniniform teeth. Typically only one caniniform tooth is present, but, as in the maxilla, some specimens do possess two. The postcaniniform teeth are mediolaterally flattened and recurved, and are generally smaller than their maxillary counterparts.

Where the large caniniform teeth insert, the dentary becomes swollen and bulges laterad. The lateral surface in this area is rugose (Fig. 29A). In the same view and immediately below the tooth row, a system of fine channels and grooves marks the paths of blood vessels. The remainder of the lateral surface is relatively smooth.

In medial view (Fig. 29B) the mandibular symphysis covers most of the surface below and anterior to the

TABLE 2—List of UCMP dentaries and their tooth counts. Abbreviations as in Table 1.

TABLE 2.

UCMP Specimen No.	R/L	Age	C/I	Precaniniforms	Caniniforms	Postcaniniforms	TOTAL
34195	L	Ad.	C	1	2	18	21
34197 (5 fragmentary specimens)							
34218	L	Ad.	C	1	2	23	26
83459	R	Ad.	C	1	2	20	23
83459	L	Ad.	I	1	2	19+	22+
83460	L	Ad.	C	1	2	20	23
83461	R	Ad.	C	1	2	20	23
83462	L	Sub.	C	1	2	17	20
83463	L	Ad.	I	?	?	18+	18+
83464	R	Ad.	C	1	2	21	24
83465	L	Ad.	I	1	2	14+	17+
83466	R	Ad.	I	1	2	19	22
83467	R	Ad.	I	1	2	17+	20+
83468	L	Ad.	C	1	2	19	22
83469	L	Sub.	I	1	2	21+?	24 (+)?
83470	R	Ad.	I	1	2	17+	20+
83471	R	Ad.	C	1	2	20	23
83472	R	Ad.	I	1	2	17+	20+
83473	L	?	I	?	?	12+	12+
83474	R	Sub.	I	1	2	9+	12+
83475	L	Ad.	I	?	?	12+	12+
83476	R	Ad.	C	1	2	21	24
83477	R	Ad.	C	1	2	22	25
83477	L	Ad.	I	1	2	?	3+
83478	R	Ad.	C	1	2	21	24
83479	R	Ad.	C	1	2	22	25
83480	R	Ad.	I	?	?	18+	18+
113150	—	Ad.	I	1	2	17+	20+

first caniniform tooth. It is bisected by the anterior extension of the meckelian canal. The alveolar ridge forms a prominent shelf posterior to the symphysis that extends back to the position of the last dentary tooth. The medial surface of the shelf is marked by vessel scars, and scars delineating the extent of contact with the anterior and posterior coronoids and the splenial. Tooth implantation along the dorsal surface of the shelf is subthecodont. The alveolar shelf forms the dorsal roof of the meckelian canal; its ventral surface is smooth and marked by occasional nutritional foramina. The remainder of the medial surface of the dentary is heavily scarred, marking the limits of contact with the angular, splenial, and surangular.

Splenial (10 specimens)

Fig. 30A shows the splenial in medial view. The symphyseal region of the element is clearly offset from the body of the element and is easily distinguished by its roughened surface. Unlike the symphyseal portion of the dentary, the splenial symphysis projects mediad 2-3 mm from the body of the element (Fig. 30C).

In lateral view (Fig. 30B) the element displays sutural surfaces for the dentary and the angular. A channel bisects the sutural surface for the dentary, thus marking the path of the meckelian canal as it passes forward to the symphysis.

Coronoids (1 specimen of each)

The coronoids are the most rarely preserved lower-jaw elements and are only known from an articulated specimen (UCMP 83459). The anterior coronoid (Fig. 31A) is the less robust of the two and extends along the medial surface of the alveolar shelf from the first postcaniniform tooth to the 16th or 17th postcaniniform tooth, where it pinches out beneath the posterior coronoid. The posterior coronoid (Fig. MB) continues back along the medial surface of the alveolar shelf to the anterior border of the meckelian fossa. Above the meckelian fossa it contacts the anterior edge of the surangular and extends dorsad to form a small coronoid process. Pits and striae along this process may indicate that some of the adductor musculature inserted here.

Surangular (22 specimens)

The surangular forms the posterodorsal portion of the mandible. In lateral view (Fig. 32A) the surangular is largely covered by the sutural surface for the dentary. Along the ventrolateral border, the sutural surface for the angular continues forward from the posterior end of the element three-quarters of the length of the element. The intersection of the sutural surfaces for the dentary and angular demonstrates that the dentary overlies the angular. Above the sutural surface for the angular, the surface of the surangular is slightly rugose and marked with grooves that continue onto the angular ventrally (see below).

In medial view (Fig. 32B) a large knob-like process that ends in unfinished bone rises above the body of the element. A small foramen pierces the knob ventrally. Behind the process, sutural scars mark the area of contact with the articular. In articulated specimens

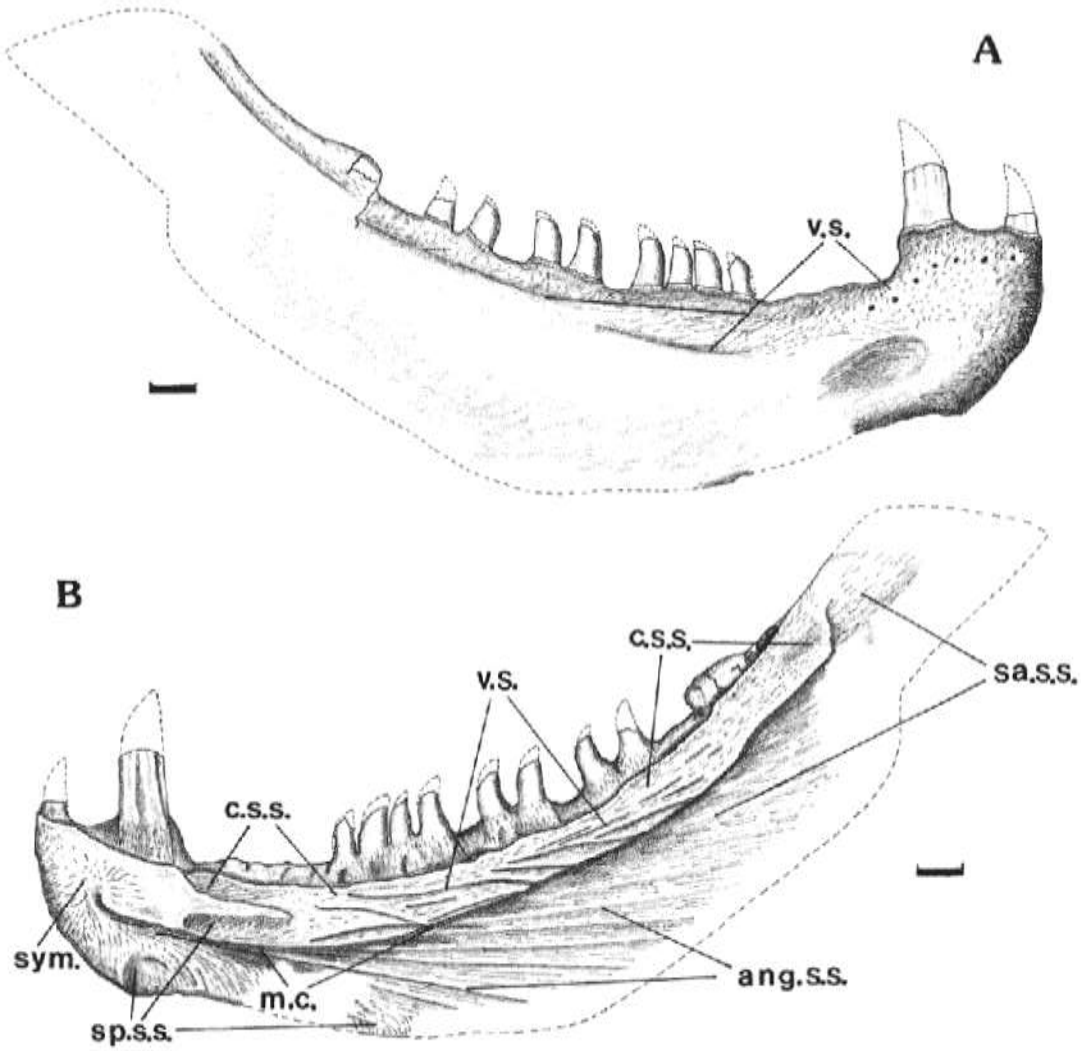

FIGURE 29—*S. ferocior*. Right dentary (UCMP 83478): **A**, lateral view; **B**, medial view. Abbreviations: **ang.s.s**, sutural surface for angular; **c.s.s.**, sutural surface for coronoids; **m.c.**, meckelian canal; **sym.**, symphysis; **sa.s.s.**, sutural surface for surangular; **sp.s.s.**, splenial sutural surface; **v.s.**, vessel scar. Scale equals 1 cm.

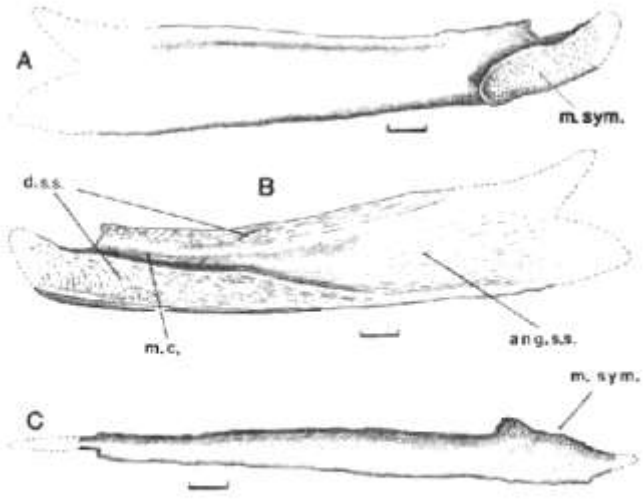

FIGURE 30—*S. ferocior*. Left splenial (UCMP 34201): **A**, medial view; **B**, lateral view; **C**, ventral view. Abbreviations: **ang.s.s.**, sutural surface for angular; **d.s.s.**, sutural surface for dentary; **m.c.**, meckelian canal; **m.sym.**, symphysis. Scale equals 1 cm.

the articular contacts the surangular only in this basined area; a cartilaginous contact probably also occurred between the knob-like process and the articular.

Anterior to this region, the meckelian fossa covers much of the medial surface of the surangular. Some scarring of the element in the fossa may indicate an area of attachment for the adductor musculature.

Angular (21 specimens)

The angular is an elongate, flattened bone that contributes to the posteroventral portion of the mandible. The anterior portion of the element is covered with sutural scars both medially and laterally so that, in articulation, only the posterior half of the element is exposed. In lateral view (Fig. 33A) an extensive sutural scar covering the anterior portion of the element marks the area of firm contact with the dentary. Posterior to the dentary contact the surface of the bone becomes rugose, channeled and slightly pitted in areas, indicating contact with skin and blood vessels. Lo-

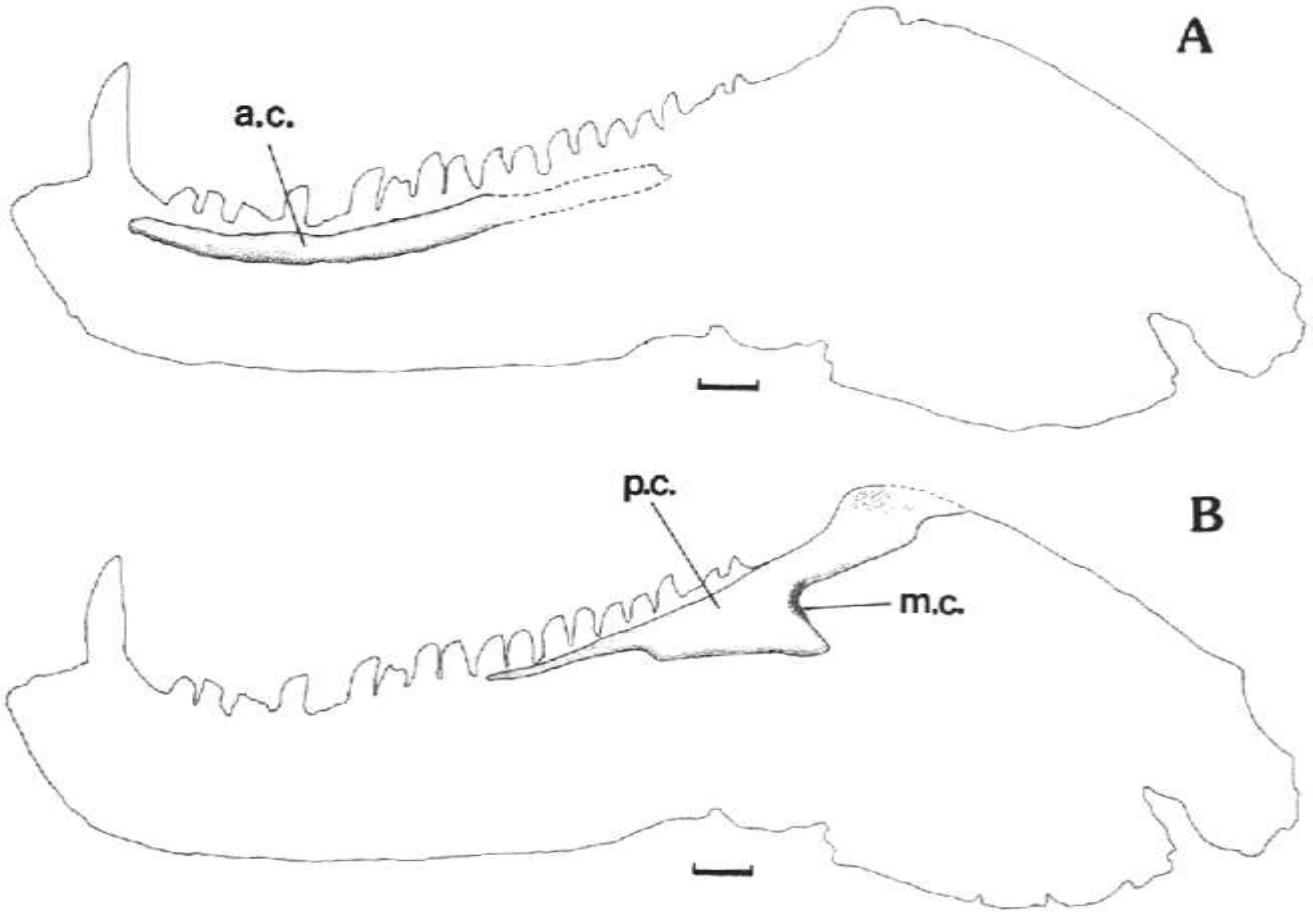

FIGURE 31—*S. ferocior*. Right coronoids (UCMP 83459): **A**, anterior coronoid, medial view; **B**, posterior coronoid, medial view. Abbreviations: **a.c.**, anterior coronoid; **m.c.**, meckelian canal; **p.c.**, posterior coronoid. Scale equals 1 cm.

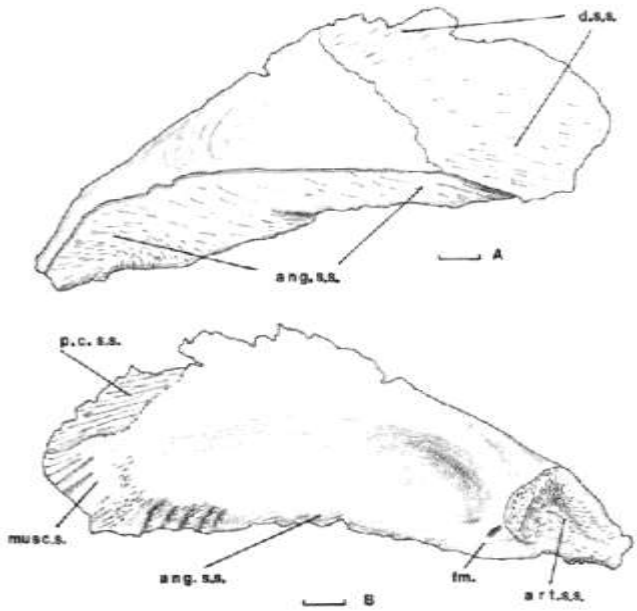

FIGURE 32—*S. ferocior*. Right surangular (UCMP 83378): **A**, lateral view; **B**, medial view. Abbreviations: **ang.s.s.**, sutural surface for angular; **art.s.s.**, sutural surface for articular; **d.s.s.**, sutural surface for dentary; **fm.**, foramen; **musc.s.**, muscle scar; **p.c.s.s.**, sutural surface for posterior coronoid. Scale equals 1 cm.

calized areas of pitting are present on the lateral surface of the reflected lamina, but the channeling is reduced. The ventral edge of the lamina is thickened and pitted. The medial surface of the lamina is smooth except for a small, anteroventrad-sloping ridge that is marked with extensive pitting. Above the reflected lamina the angular folds back down upon itself and forms a notch at the posterior end. Apparently, this notch accommodated the pterygoideus musculature that runs between the pterygoid and the articular.

Below the anterior portion of the meckelian canal a large, wedge-shaped sutural surface marks the area where the splenial contacts the angular. Posterior to the meckelian canal and lying immediately above the smooth medial face of the reflected lamina is the sutural surface for the prearticular. It is a narrow, shallow basin that extends back to a position above the notch. Posterior to this area a thin lamina of the angular forms the sutural surface for the lateral face of the articular. Above this area sutural scars mark the extent of the contact with the surangular.

Prearticular (3 specimens)

The prearticular (Fig. 34) is a narrow, twisted element that runs from the anterior edge of the articular

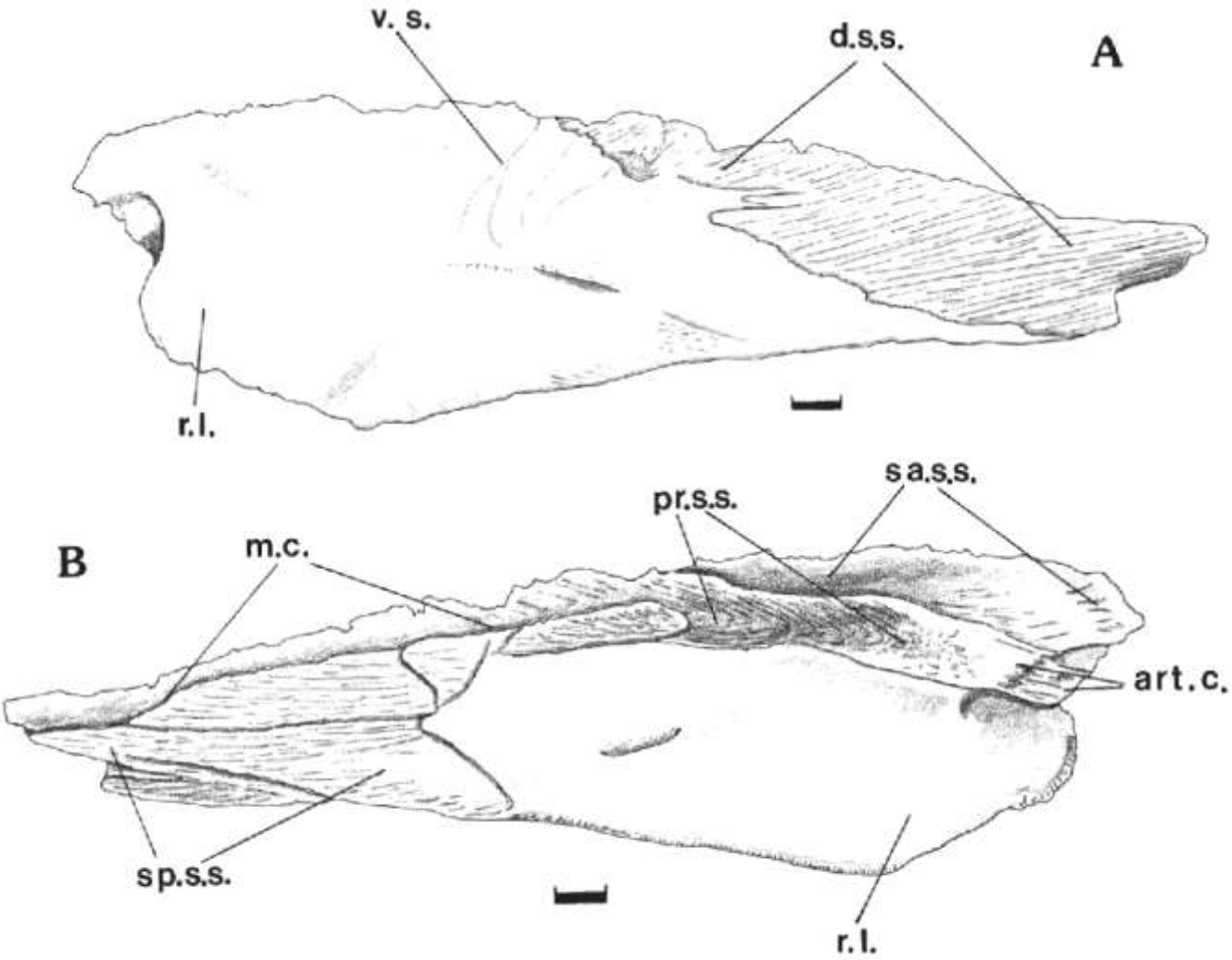

FIGURE 33—*S. ferocior*. Right angular (UCMP 83397): **A**, lateral view; **B**, medial view. Abbreviations: **art.c.**, contact point of articular; **d.s.s.**, sutural surface for dentary; **m.c.**, meckelian canal; **pr.s.s.**, sutural surface for prearticular; **r.l.**, reflected lamina; **sa.s.s.**, sutural surface for surangular; **sp.s.s.**, splenial sutural surface; **v.s.**, vessel scar. Scale equals 1 cm.

to beneath the posterior coronoid. The contact between the prearticular and the articular is complex; the anterior edge of the articular is wedged into the posterior end of the prearticular so that the anteromedial and anterolateral faces of the articular are covered by the prearticular. Running forward from the articular, the prearticular is markedly twisted and forms the floor of the meckelian fossa. Farther forward, a small lamina or crest projects dorsomediad and forms a portion of the medial wall of the meckelian canal. The ventral edge of the prearticular contacts the angular and continues forward to gain a contact with the dorsal edge of the splenial.

Articular (20 specimens)

The articular is a small, massive bone at the posterior corner of the mandible. In medial view (Fig. 35A) the two condylar recesses face anterodorsomediad. Their long axes are subparallel and converge just in front of the element. The anteromedial edge of the articular contacts the prearticular. The lateral surface is divided into two regions: a dorsal sutural surface for the surangular, and a ventral sutural surface for the prearticular and the angular. The area of contact with the surangular is the more extensive of the two. Lightly scarred areas anteroventrally and centrally mark the limits of the prearticular and angular contacts, respectively. Along the posterior surface is a small retroarticular process. In few specimens is the process fully preserved. A broad, ventrad projecting pterygoideus process is visible in either view. The process is heavily scarred on its medial surface, indicating the limit of pterygoideus-muscle insertion.

Comparisons

The genus *Sphenacodon* contains two species: the smaller type species *S. ferox* erected by Marsh (1878) and the larger *S. ferocior* erected by Romer (1937). The type of *S. ferocior* was described by Romer (1937) as "A form similar to S. *ferox* in all major morphological features but 50 per cent larger than the type species." Romer and Price (1940) cited differences between the two species as follows: 1) Adults of S. *ferox* are 2040% smaller than those of *S. ferocior* and possess a more slender build, less exaggerated neural spines,

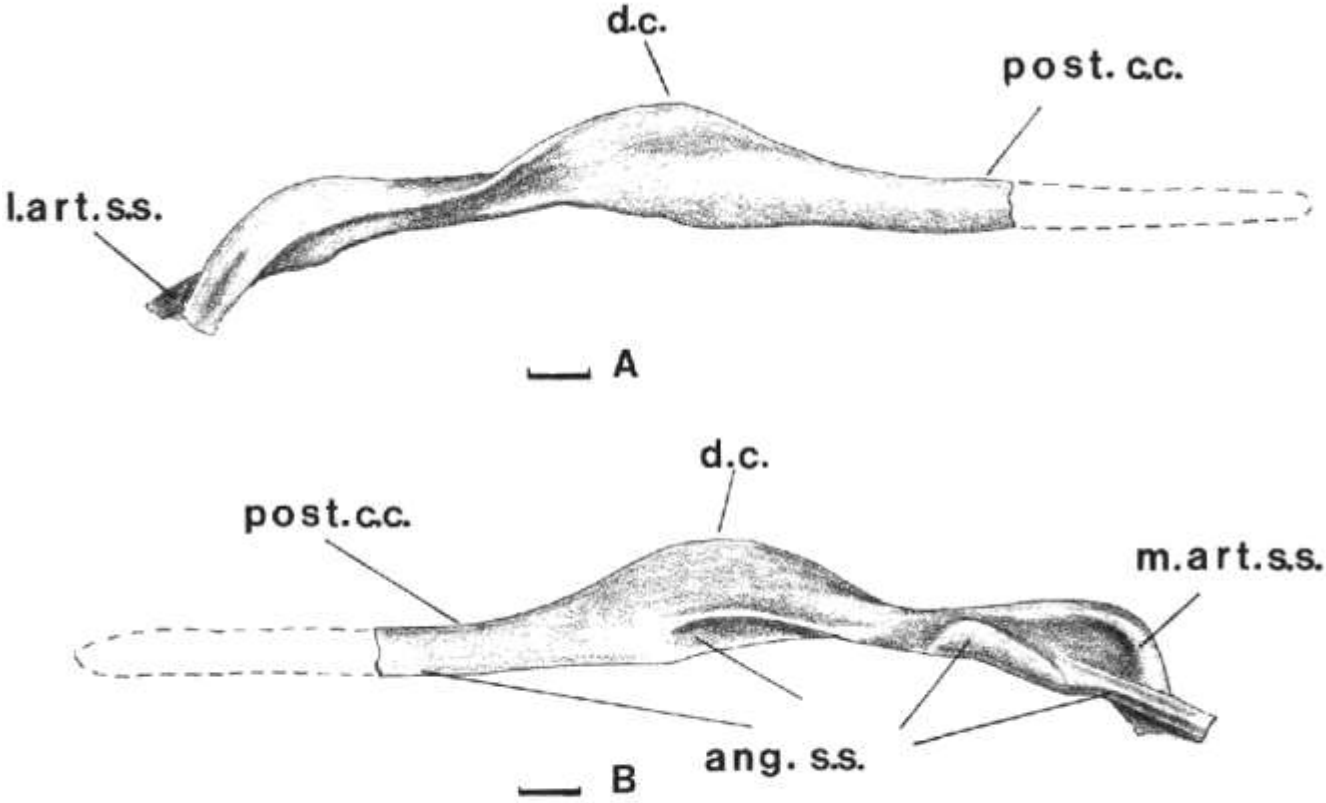

FIGURE 34—*S. ferocior*. Left prearticular (UCMP 34218): **A**, lateral view; **B**, medial view. Abbreviations: **ang.s.s.**, sutural surface for angular; **d.c.**, dorsal crest; **l.art.s.s.**, sutural surface for lateral surface of articular; **m.art.s.s.**, sutural surface for medial surface of articular; **post.c.c.**, area of contact of posterior coronoid. Scale equals 1 cm.

less rugose skull, lighter supraorbital roof, and relatively larger orbits and temporal openings; 2) maxillary "step" is less developed in S. *ferox;* 3) maxillary tooth row is less convex in *S. ferox;* 4) the quadrate region is more pendant in *S. ferox.* Langston (1952) cited a relatively unreduced tooth count in *S. ferox as* a further difference.

Langston (1952) tentatively referred the Anderson quarry *Sphenacodon to S. ferocior* on the basis of its large size. While study of the Anderson quarry material has demonstrated the presence of elements whose sizes correspond closely to those of the type of *S. ferocior (MCZ* 1489), a minor difference in the tooth counts exists. The total maxillary-tooth count in the type of S. *ferocior* is 14 and consists of 0 precaniniform, 2 caniniform, and 12 postcaniniform teeth. Maxillary-tooth counts in the Anderson quarry *Sphenacodon* range from 15 to 20 and consist of 0-4 precaniniform, 2 caniniform, and 12-15 postcaniniform teeth. The combination of 12 postcaniniform and 0 precaniniform teeth seen in the type is closely approached in two Anderson quarry *Sphenacodon* specimens that have 12 postcaniniform and 1 precaniniform teeth each. All other Anderson quarry specimens with 12 postcaniniform teeth possess either 2 or 3 precaniniform teeth. Conversely, the two Anderson quarry specimens that have 0 precaniniform teeth possess a minimum of 14 postcaniniform teeth.

It was noted above that postcaniniform-tooth counts increase and precaniniform-tooth counts decrease during ontogeny. The maxillary-tooth count in the type of *S. ferocior* (an obvious adult) suggests that the postcaniniform-tooth count in this form might be less at comparable ontogenetic stages than in the Anderson quarry individuals. However, the maxillary-tooth-count data from the Anderson quarry (Table 1) also underscore the fact that variation in tooth counts at different ontogenetic stages can be large. Because of the absence of a sample population of *S. ferocior* from the type locality and the close correspondence in size between the type and the largest specimens in the Anderson quarry collection, referral of the Anderson quarry *Sphenacodon* material to S. *ferocior* appears justifiable for the time being.

Apart from size, however, the distinctions cited above between S. *ferox* and S. *ferocior* (using the Anderson quarry material for comparison) are not pronounced. The convexity of the maxillary tooth row and the degree of development of the maxillary "step" are both ontogenetically variable in the Anderson quarry material. Fig. 36 shows representative outline drawings of maxillae of both S. *ferox* (based upon a sample of 7) and S. *ferocior* (based upon a sample of 13). Visual inspection indicates that the degree of convexity of the alveolar ridge increases with size in both species. Furthermore, maxillary "step" development, as discussed above in the description of the maxilla, also increases with size. It is clear from Fig. 36 that the "step" in front of the first caniniform tooth corresponds fairly well in most of these specimens. Only in the smallest specimen of *S. ferocior* is this "step" poorly developed.

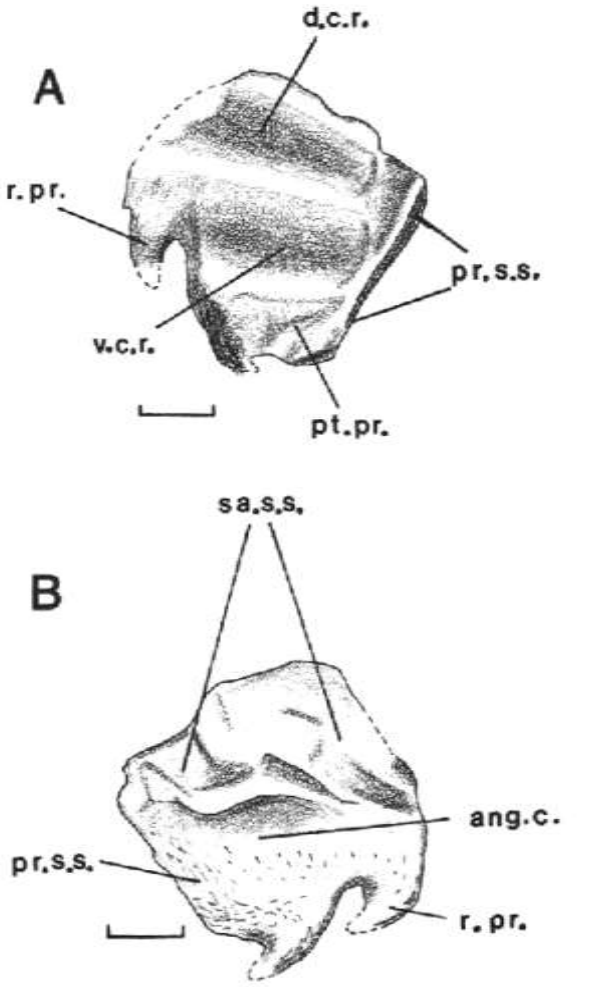

FIGURE 35—*S. ferocior.* Left articular (UCMP 34202): A, medial view; B, lateral view. Abbreviations: **ang.c.**, area of contact of angular; **d.c.r.**, dorsal condylar recess; **pr.s.s.**, sutural surface for prearticular; **pt.pr.**, pterygoideus process; **r.pr.**, retroarticular process; **sa.s.s.**, sutural surface for surangular; **v.c.r.**, ventral condylar recess. Scale equals 1 cm.

Regarding the differences in the quadrate region, Romer and Price (1940) tempered their observations stating that ". . . this last character may be due to imperfections present in this region." This statement was in reference to the type of *S. ferocior* where the quadrate was thought to be less pendant than in *S. ferox.* Examination of the type shows that this area is disarticulated and, therefore, of little value in determining the degree of pendancy. Study of the disarticulated specimens from the Anderson quarry offers no clearer idea on this subject.

Langston's reference to an unreduced dentition in *S. ferox* relative to *S. ferocior* notes: 1) The occurrence of two premaxillary teeth in two of 18 premaxillae of *S. ferocior* (one from the Anderson quarry and one from an unknown locality near Arroyo de Agua) as opposed to three premaxillary teeth in all known specimens of *S. ferox;* 2) a relatively smaller third premaxillary tooth in at least one-half of the premaxillae from Anderson quarry; 3) relatively smaller precaniniform teeth in *S. ferocior* (where precaniniform teeth are present).

While Langston's criteria may certainly underscore important trends in the diversification of *Sphenacodon* morphology during the Early Permian, their use as diagnostic characters are compromised by significant variation in tooth-count numbers and relative tooth development. Thus, they cannot be applied in the absence of large samples.

On the basis of size differences alone, however, separation of the known *Sphenacodon* material into two species is currently justified. It is anticipated that future discoveries will produce forms of intermediate size, however.

S. ferocior and *"Oxyodon" brittanicus*

A single sphenacodontine maxilla and counterpart from the English midlands known previously as *Oxyodon brittanicus* was referred to *Sphenacodon* by Paton (1974) after she noted that the former generic name was preoccupied by a genus of acropomatid fish. Citing similar size, proportions, and relative caniniformtooth development as in S. *ferox,* Paton referred the specimen to that genus and retained the specific name *brittanicus as* a geographic convenience. On the basis of these criteria, however, referral to *Dimetrodon booneorum* appears to be equally justified. Until better material of the form is retrieved from this region, *"Oxyodon" brittanicus* should be considered Sphenacodontinae incertae sedis.

Sphenacodon and *Dimetrodon*

Romer and Price (1940, p. 322) revised the diagnosis of *Sphenacodon* as follows:

> ". . . similar . . . in . . . general structure to the short-bodied species of *Dimetrodon* in the Wichita beds of Texas; differing, however, in a slightly less pronounced specialization of the dental battery and more especially in the fact that the sail was absent, the neural spines being somewhat elongate but retaining their normal pelycosaurian shape."

The differences pertaining to the dental battery are questionable, however, as Romer and Price state (p. 323):

> "In the marginal *teeth* 3 or 2 premaxillary incisors, about 14 to 16 maxillaries including 12 postcanines and 2 to 0 precanines, and 22 to 24 dentary teeth appear to be typical numbers. This count is essentially the same as the average *Dimetrodon. . . .* on the whole the genus is as advanced in dental development as the average Wichita *Dimetrodon."*

No other references to specializations or lack thereof in the dental battery are made. The preceding description of *S. ferocior* from the Anderson quarry has demonstrated a more variable tooth count than is described by Romer and Price (1940). Comparisons of this modified tooth count with those of different species of *Dimetrodon* suggest no means for generic separation.

Romer and Price also cited differences in skull proportions and in the position of the jaw articulation between these two genera. They claimed that, relative to estimated body weight, the postorbital skull length is greater in *Sphenacodon* than in *Dimetrodon.* They employed the orthometric linear unit (see Romer and Price, 1940, p. 7, for its application in pelycosaurs) as

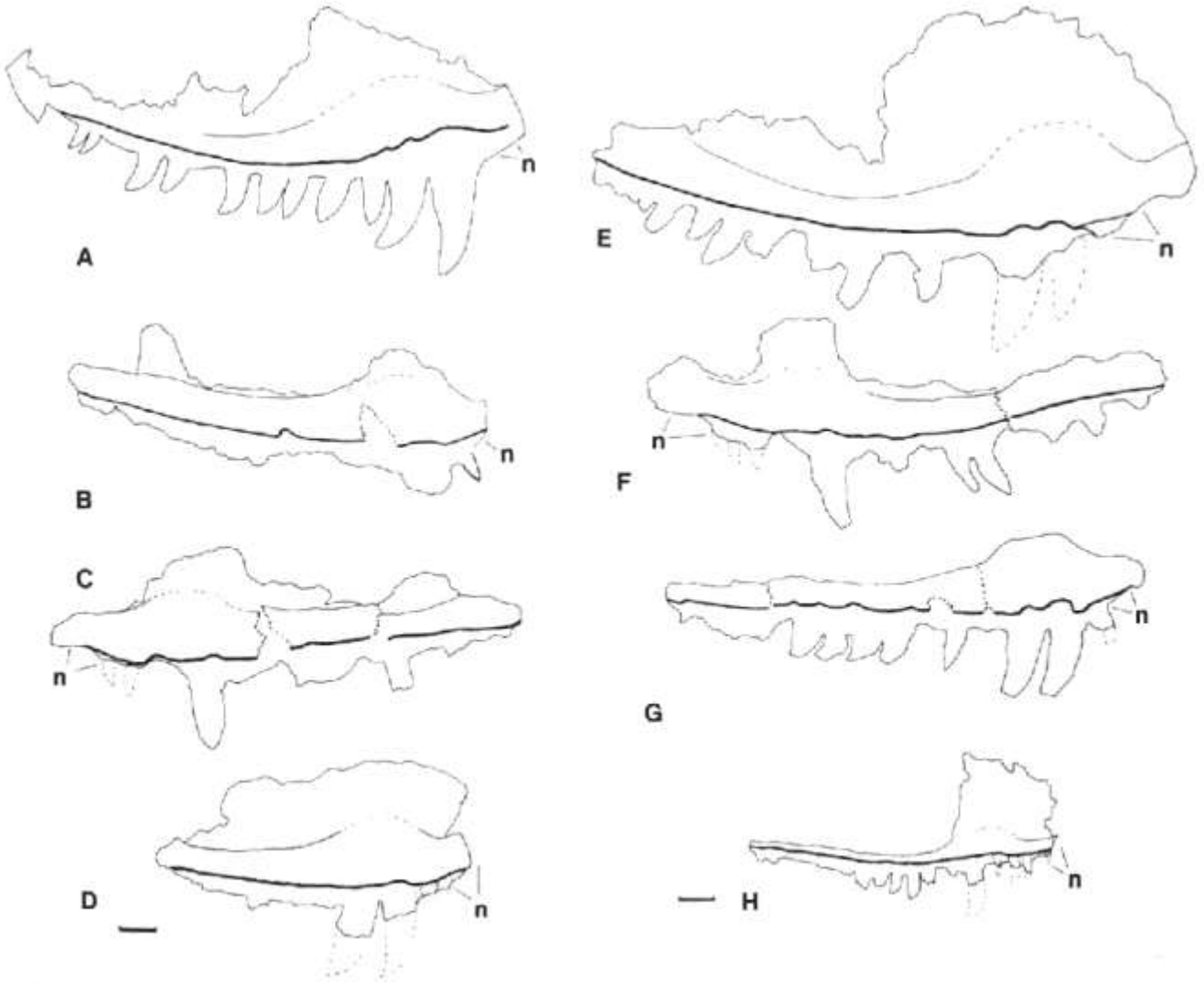

FIGURE 36—*S. ferox* **(A–D)** and *S. ferocior* **(E–H).** Some maxillae that demonstrate increased convexity of alveolar ridge associated with increasing ontogenetic development. **A,** Adult; **B–G,** subadult; **H,** juvenile. Scale equals 1 cm.

a means of determining the proportional difference. However, the postorbital skull length and associated dorsal-centrum measurements necessary to calculate these proportions are derived from a crushed and reconstructed (plaster) skull (W.M. 35) associated with laterally flattened vertebrae, and a disarticulated postorbital region from the type of *S. ferocior* (MCZ 1489) that is not associated with any dorsal vertebrae. The proportions they list for these two specimens are not that different from those of *D. limbatus* (compare 13.2 and 17.8 for *D. Iimbatus,* and 18.6 for S. *ferocior* and 19.4 for *S. ferox).* Slight underestimates of centrum width (1-2 mm) or overestimates of postorbital skull length (10-15 mm) could easily account for these differences. When the preservation is considered, this character becomes suspect.

Romer and Price tentatively suggested that the jaw articulation might be lower relative to the tooth row in *Sphenacodon.* The *Sphenacodon* material from the Anderson quarry shows two orientations in the shape of the cheek region. In one form the posterior process of the jugal is strongly downturned, resulting in a lower position of the articular region of the skull (Fig. 3B). In the other form the posterior process is less downturned and a *Dimetrodon-like* position of the articular region is inferred (Fig. 3A). Thus, the utility of this character as a diagnostic tool is compromised by its variable occurrence.

Below is a discussion of those cranial elements of *S. ferocior* whose morphology as described in this paper appears to differ appreciably from *Dimetrodon limbatus* as figured by Romer and Price (1940).

The septomaxillary process of the nasal in *Sphenacodon ferocior* (Fig. 6) appears much wider than in *D. limbatus.* Also, there is no indication in either view that the septomaxillary process formed the dorsal border of the septomaxillary foramen, as appears to be the case in *D. limbatus.* Finally, the nasal—maxilla contact appears to be more extensive in *D. limbatus,* with a concomitant reduction of the nasal—lacrimal contact and the anterior extent of the lacrimal. Articulated remains of *S. ferocior* demonstrate the wide septomaxillary process, but do not preserve the septomaxillary foramen well enough to clarify whether or not the nasal borders it dorsally. Reconstructions of skulls pertaining to different species of *Dimetrodon* (Romer

and Price, 1940, fig. 5) show a wide septomaxillary process of the nasal developed in *D. milleri.* A discussion of this character is lacking; however, since it is present in at least one species of *Dimetrodon,* it cannot be used as a generic character for *Sphenacodon.*

The maxilla–nasal contact is consistently well developed in all species of *Dimetrodon* and always exceeds the nasal–lacrimal contact. While the opposite condition is always present in *S. ferocior,* the nature of these contacts is unknown in *S. ferox.* Williston (1918) reconstructed *S. ferox* (W.M. 35) with a *S. ferocior-like* arrangement, but examination of this material shows that most of the important areas have been covered with plaster during the restoration of the specimen. The arrangement is not determinable in other specimens of *S. ferox,* but it seems reasonable that this form, which did not possess highly developed caniniform teeth, should retain an essentially primitive arrangement of the type seen in S. *ferocior.*

The vomer of S. *ferocior* (Fig. 19) shows an additional groove on the medial surface of the element that has not been described or figured in any specimen of *Dimetrodon.* It might represent a line of contact between the paired vomers, a vessel track, or it may simply be the result of distortion or overpreparation. Its apparent absence in *Dimetrodon* is not surprising, however, given the lack of isolated vomers in that genus. At any rate, given the occurrence of only one pair of poorly preserved vomers in S. *ferocior,* this character should be regarded as insufficient to warrant generic separation.

The palatine in S. *ferocior* appears to switch its contact from the ventrolateral to the dorsolateral surface of the pterygoid at the midlength of the palatine (Fig. 20). All indications in *D. limbatus are* that the palatine retains a contact on the dorsolateral surface of the pterygoid along its entire length. However, in none of the four palatines of *S. ferocior* from the Anderson quarry are these surfaces fully preserved. Thus, this interpretation of a switching contact remains tentative.

The descriptions and figures of the sphenethmoids of S. *ferocior* and *D. limbatus* are different enough to warrant discussion. Romer and Price (1940, p. 78) described the sphenethmoid of *D. limbatus* as follows:

> "Between the median septum and the diverging lateral walls of the trough there is on either side a pair of grooves leading forward and somewhat downward and outward. The more medial groove of each pair is the more ventral; in *Dimetrodon* this groove is separated by *a* bar of bone from its dorso-lateral neighbor, so that its opening has become a foramen. The dorso-lateral opening is also a foramen, since the groove through which it opens is roofed by the frontal."

Fig. 37 shows the Romer and Price reconstruction of this element with the significant areas labeled in the terminology of this paper. In *S. ferocior* the dorsolateral grooves are covered by bone as shown in Fig. 27B. Examination of the figured *D. limbatus* sphenethmoid MCZ 1347 suggests that this was also the case in that specimen. Fig. 38 shows MCZ 1347 unreconstructed and in right-lateral view. Immediately obvious are the two grooves separated by a horizontal bar of bone. The dorsolateral groove has been crushed

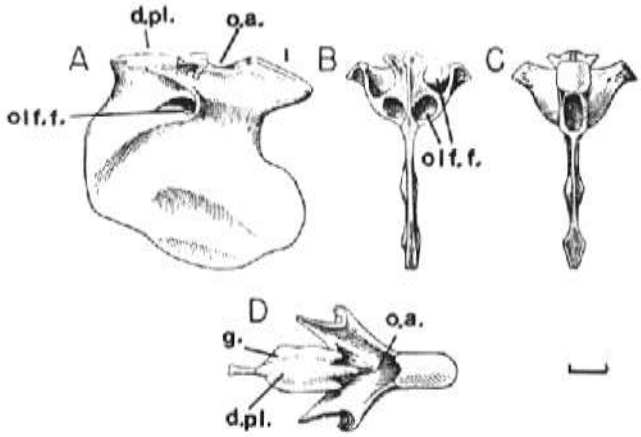

FIGURE 37—*Dimetrodon limbatus.* Sphenethmoid (MCZ 1347): **A,** lateral view of left side; **B,** anterior view; **C,** posterior view; **D,** dorsal view. From Romer and Price (1940). Abbreviations as in Fig. 27. Scale equals 1 cm.

medially, but the remains of a bony roof above the "groove" are still visible. The left side of the specimen is covered by a fragment of unidentifiable bone, preventing further examination. Examination of less well preserved sphenethmoids of *Dimetrodon* in the MCZ collection corroborates this newer interpretation. Thus, the morphology of the sphenethmoid in *Dimetrodon limbatus is identical* to that in S. *ferocior.*

Sphenacodon and *Ctenospondylus*

Vaughn (1964) reported the first discovery of an articulated skull referable to the sphenacodontine *Ctenospondylus (aff. C.* casei)—previously known only from postcrania—from the Organ Rock Shale of the Cutler Group of southeast Utah. After comparing this skull (NTM VP 1001) with *Sphenacodon* and *Dimetrodon,* Vaughn concluded that, superficially, the skulls of these three genera were indistinguishable. Citing differences in the sphenethmoid and parasphenoidal rostrum, however, he expounded a means of separating *Ctenospondylus* from *Sphenacodon* and *Dimetrodon.* He listed differences in five regions of the sphenethmoid between *Ctenospondylus* and *Dimetrodon,* but could only apply two of these to *Sphenacodon* due to imperfections in the *Sphenacodon* material.

His description and figures of the morphology of the olfactory foramina in *Ctenospondylus* are identical to that which has been presented above for S. *ferocior* (Fig. 27) and *D. limbatus* (Fig. 38). He was unaware of the misinterpretation in Romer and Price (1940), and the superficial resemblance of the poorly prepared *Sphenacodon* sphenethmoid, UCMP 34218, to that of *D. limbatus* figured by Romer and Price compounded the error. Thus, the arrangement of olfactory foramina in all three taxa is identical.

Secondly, he stated that the angle of the posterior tip of the dorsal plate (dorsal view) is perhaps more obtuse in *Ctenospondylus* than in the other two taxa. Examination of sphenethmoids of the three taxa strongly suggests that the posterior end of the dorsal plate in *Ctenospondylus* has not been preserved. In *Dimetrodon* and *Sphenacodon* the narrow posterior end

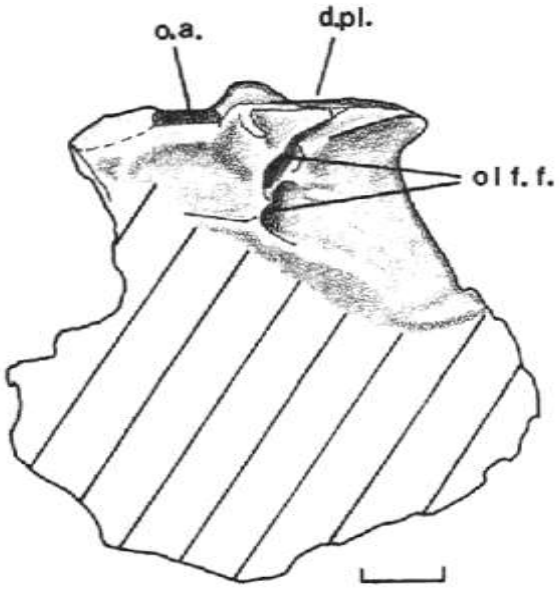

FIGURE 38—*Dimetrodon limbatus*. Sphenethmoid (MCZ 1347), lateral view of left side. Abbreviations as in Fig. 27. Scale equals 1 cm.

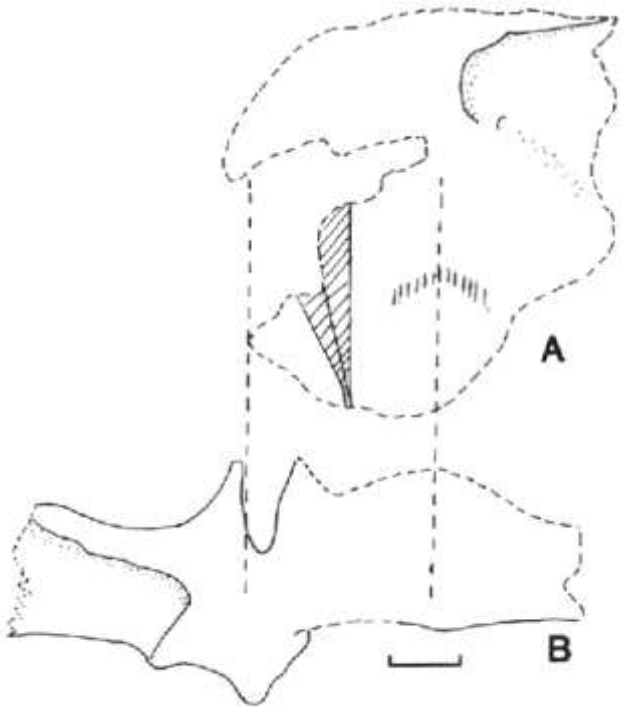

FIGURE 39—*Ctenospondylus* cf. *casei*. **A**, Sphenethmoid (NTM VP 1001), left side; **B**, basiparasphenoid (NTM VP 1001), left side. Scale equals 1 cm.

of the dorsal plate extends back as far as the midpoint of the lateral processes. In *Ctenospondylus* the dorsal plate terminates well ahead of the lateral processes as a blunt, broad surface. If the narrow posterior portion of the plate was not preserved in *Dimetrodon* or *Sphenacodon,* the shape of the end of the plate and its position relative to the lateral processes would be identical to that seen in *Ctenospondylus.*

The three remaining differences between the sphenethmoid of *Ctenospondylus* and *Dimetrodon* involve regions that are lacking in S. *ferocior* specimens and, therefore, cannot be evaluated in the latter taxon. Inspection of the sphenethmoids of both *Ctenospondylus* and *Dimetrodon* indicates that these are admittedly "minor" differences that involve regions in the *Ctenospondylus* specimen where poor preservation may have significantly altered the region in question. The three characters are listed below as they occur in *Ctenospondylus* relative to *D. limbatus:* (1) incomplete ossification between the two olfactory foramina on either side of the sphenethmoid; (2) acute shape in the notch in the posterior edge of the sphenethmoid; (3) lack of a plate of bone covering the median trough posteriorly.

Vaughn (1964) also observed a difference between *Ctenospondylus,* and *Sphenacodon* and *Dimetrodon* in the lateral outline of the dorsal edge of the cultriform process immediately posterior to the contact with the sphenethmoid. He stated that in *Ctenospondylus* the dorsal outline is convex a short distance anterior to the sella turcica, whereas in *S. ferocior* and *D. limbatus* it is concave. Fig. 39 shows both the sphenethmoid and parasphenoid of *Ctenospondylus.* It is obvious from this associated parasphenoid—sphenethmoid pair that the actual point of contact between the two elements must occur farther forward to prevent the sphenethmoid from resting in the sella turcica. However, incomplete preservation of the rostrum makes a re-evaluation of its true dorsal outline impossible. Thus, this character appears of little value in distinguishing among these taxa.

Examination of the *Ctenospondylus cranial* material (NTM VP 1001) has not brought to light any other characters that cannot be matched in *S. ferocior.* However, it is important to note that NTM VP 1001 possesses both a strongy downturned posterior process of the jugal and a nasal—lacrimal contact that is greater in extent than the nasal—maxilla contact, two features that are known in *Sphenacodon* but absent in *Dimetrodon.*

Sphenacodon and *Bathygnathus, Neosaurus,* and *Macromerion*

Bathygnathus* Leidy (1854) is known from one specimen from the red beds of Prince Edward Island, a partial articulated snout. The size, tooth count, development of the maxillary "step" and alveolar convexity all indicate that *Bathygnathus* is indistinguishable from either *D. limbatus* or *S. ferocior.

***Neosaurus* Nopsca (1923) is represented by a small partial maxilla from the Autunian deposits near Paris, France. It displays four precaniniform teeth, a slight maxillary "step," and only 10 postcaniniform teeth. It has been noted above (Fig. 36H) that the Anderson quarry contains at least one juvenile maxilla of *S. ferocior* that shows a precaniniform-tooth count of four, an undeveloped maxillary "step," and a relatively straight alveolar ridge. In addition, it has been suggested that during ontogeny precaniniform-tooth counts decrease, while postcaniniform-tooth counts increase. Thus, *Neosaurus* may represent a juvenile**

sphenacodontine very closely related to *Sphenacodon, Dimetrodon,* or *Ctenospondylus.*

Macromerion Fritsch (1879) consists of cranial and few postcranial fragments that display typical sphenacodontid features such as an enlarged caniniform-tooth buttress on the inside of the maxilla and enlarged, subquadrate, caniniform-tooth bases. Romer (1945) compared this material with *Dimetrodon,* but in the absence of neural spines declined to refer the specimens to any of the better known taxa.

Discussion

Although no major morphological differences in cranial morphology have been cited as a means of distinguishing between the two recognized species of *Sphenacodon,* differences in the relative size of elements still provide a reliable means of placing the known specimens within one or the other species. Within the entire skeleton, differences in the relative development of the neural spines are the most pronounced and still offer a means of quantifying these size differences (see Romer and Price, 1940). However, it is to be expected that future discoveries will produce specimens that are intermediate in size.

The skulls of *Sphenacodon ferocior* and *Ctenospondylus* a ff. *casei* can tentatively be distinguished from those of *Dimetrodon* by a nasal-lacrimal contact that is primitively equal to, or greater than, the nasal-maxilla contact. *Dimetrodon* displays a derived, extensive nasal-maxilla contact that is always greater than the nasal-lacrimal contact. This difference should be cautiously applied, however, until the nature of these contacts can be established in *S. ferox* and *Ctenospondylus ninevehensis* (Berman, 1978). Caution is also advised in anticipation of future discoveries of more advanced *Sphenacodon* and *Ctenospondylus* specimens that may possess a *Dimetrodon-like* arrangement, or more primitive *Dimetrodon* specimens possessing *a Sphenacodon*like arrangement.

Sphenacodon and *Ctenospondylus* share the derived characters of a strongly downturned posterior process of the jugal (not consistently developed in *Sphenacodon)* and elongate, laterally flattened neural spines. At present, no cranial differences can be cited to distinguish between the two taxa. In fact, work in progress suggests that the postcranial differences in the relative development of the neural spines are probably not significant enough to warrant generic separation, if ranges of spine-height development seen in *Dimetrodon are* adopted as a comparative standard. Further study of the postcranial skeletons is now necessary to test this hypothesis.

"Oxyodon," Bathygnathus, Neosaurus, and *Macromerion* are clearly sphenacodontids by virtue of the presence in each of an enlarged, smoothly contoured caniniform-tooth buttress, and an enlarged caniniform-tooth pair possessing subquadrate bases and unserrated, laterally compressed distal tips. Materials referred to *Macromerion* do not include the anterior portion of the maxilla, and it is impossible to determine whether this form was in fact a sphenacodontine. *Neosaurus, Bathygnathus,* and *"Oxyodon"* possess a maxillary "step" and are clearly sphenacodontines. While it may be argued that generic assignment of these forms is impossible on the basis of the present material, and that the names are invalid, retaining the generic names as paleogeographical convenience terms is desirable. However, the name *Oxyodon* has been shown to be preoccupied (Paton, 1974), and that material should be referred to as Sphenacodontinae incer tae sedis.

References

Barghusen, H. R., 1968, The lower jaw of cynodonts (Reptilia, Therapsida) and the evolutionary origin of mammal-like adductor jaw musculature: Postilla, no. 116, pp. 1-49.

Barghusen, H. R., 1973, The adductor jaw musculature of *Dimetrodon* (Reptilia, Pelycosauria): Journal of Paleontology, v. 47, no. 5, pp. 823-834.

Berman, D. S, 1977, A new species of *Dimetrodon* (Reptilia, Pelycosauria) from a non-deltaic facies in the Lower Permian of north-central New Mexico: Journal of Paleontology, v. 51, no. 1, pp. 108-115.

Berman, D. S, 1978, *Ctenospondylus ninevehensis,* a new species (Reptilia, Pelycosauria) from the Lower Permian Dunkard Group of Ohio. Annals of Carnegie Museum, v. 47, art. 21, pp. 493514.

Brinkman, D., and Eberth, D. A., 1983, The interrelationships of pelycosaurs: Breviora, no. 473, pp. 1-35.

Case, E. C., 1907, Revision of the Pelycosauria of North America: Publications of the Carnegie Institute (Washington, D.C.), no. 55, pp. 66-67.

Case, E. C., and Williston, S. W., 1913, A description of certain collections of bones referred to *Sphenacodon* Marsh: Publications of the Carnegie Institute (Washington, D.C.), no. 181, pp. 61-70.

Currie, P. J., 1979, The osteology of haptodontine sphenacodonts (Reptilia: Pelycosauria): Palaeontographica (A), v. 163, pp. 130- 168.

Heaton, M. J., 1979, Cranial anatomy of primitive captorhinid reptiles from the Early Permian: Oklahoma Geological Survey, Bulletin, v. 127, pp. 1-84.

Langston, W., Jr., 1952, Permian vertebrates of New Mexico: Ph.D. dissertation, University of California (Berkeley), pp. 141-153.

Langston, W., 1953, Permian amphibians from New Mexico: University of California Publications in the Geological Sciences, Bulletin, v. 29, pp. 349-416.

Leidy, J., 1854, On *Bathygnathus borealis, an* extinct saurian of the New Red Sandstone of Prince Edward's Island: Philadelphia Academy of Natural Science, Journal (2), v. 2, pp. 327-330.

Marsh, 0. C., 1878, Notice of new fossil reptiles: American Journal of Science (3), v. 15, pp. 410-411.

Nopsca, F., 1923, Die Familien der Reptilien: Fortschritte der Geologic and Palaeontologie, Heft 2, pp. 1-210.

Oelrich, T. M., 1956, The anatomy of the head of *Ctenosaura pectinata* (Iguanidae): University of Michigan Museum of Zoology, Miscellaneous Publication no. 94, 167 pp.

Paton, R. L., 1974, Lower Permian pelycosaurs from the English midlands: Palaeontology, v. 17, pt. 3, pp. 541-552.

Reisz, R. R., 1980, The Pelycosauria: a review of phylogenetic relationships; *in* Panchen, A. L. (ed.), The terrestrial environment and origin of land vertebrates: Systematics Association, Special Symposium, v. 15, pp. 553-592.

Romer, A. S., 1937, New genera and species of pelycosaurian reptiles: New England Zoological Club, Proceedings, v. 16, pp. 89-96.

Romer, A. S., 1945, The Late Carboniferous vertebrate fauna of Kounova (Bohemia) compared with that of the Texas redbeds: American Journal of Science, v. 243, pp. 417-442.

Romer, A. S.,1956, Osteology of the reptiles: University of Chicago Press, 772 pp.

Romer, A. S., and Price, L. W., 1940, Review of the Pelycosauria: Geological Society of America, Special Paper 28, 538 pp.

Smith, D. G., 1983, Anastomosed fluvial deposits: modern examples from western Canada; in Collinson, G. D., and Lewis, G. (eds.), Modern and ancient fluvial systems. International Association of Sedimentologists, Special Publication no. 6, pp. 155-168.

Vaughn, P. P., 1964, Vertebrates from the Organ Rock Shale of the Cutler Group, Permian of Monument Valley and vicinity, Utah and Arizona: Journal of Paleontology, v. 38, no. 3, pp. 567583.

Vaughn, P. P., 1970, Lower Permian vertebrates of the Four Corners and the midcontinent as indices of climatic differences: 1969 North American Paleontological Congress, Proceedings, pp. 388-408.

Williston, S. W, 1911, American Permian vertebrates: University of Chicago Press, 145 pp.

Williston, S. W., 1916, Synopsis of the American Permo-Carboniferous Tetrapoda: Contributions of the Walker Museum, v. 1, no. 9, pp. 193-236.

Williston, S. W., 1917, *Sphenacodon* Marsh, a Permo-Carboniferous theromorph reptile from New Mexico. National Academy of Science, Proceedings, v. 2, pp. 650-654.

Williston, S. W., 1918, The osteology of some American Permian vertebrates, ill: Contributions of the Walker Museum, v. 2, pp. 104-110.

Williston, S. W., 1925, The osteology of the reptiles: University of Chicago Press, 300 pp.

Selected conversion factors*

TO CONVERT	MULTIPLY BY	TO OBTAIN
Length		
inches, in	2.540	centimeters, cm
feet, ft	3.048×10^{-1}	meters, m
yards, yds	9.144×10^{-1}	m
statute miles, mi	1.609	kilometers, km
fathoms	1.829	m
angstroms, Å	1.0×10^{-8}	cm
Å	1.0×10^{-4}	micrometers, μm
Area		
in^2	6.452	cm^2
ft^2	9.29×10^{-2}	m^2
yds^2	8.361×10^{-1}	m^2
mi^2	2.590	km^2
acres	4.047×10^{3}	m^2
acres	4.047×10^{-1}	hectares, ha
Volume (wet and dry)		
in^3	1.639×10^{5}	cm^3
ft^3	2.832×10^{-2}	m^3
yds^3	7.646×10^{-1}	m^3
fluid ounces	2.957×10^{-2}	liters, l or L
quarts	9.463×10^{-1}	l
U.S. gallons, gal	3.785	l
U.S. gal	3.785×10^{-3}	m^3
acre-ft	1.234×10^{3}	m^3
barrels (oil), bbl	1.589×10^{-1}	m^3
Weight, mass		
ounces avoirdupois, avdp	2.8349×10^{1}	grams, gr
troy ounces, oz	3.1103×10^{1}	gr
pounds, lb	4.536×10^{-1}	kilograms, kg
long tons	1.016	metric tons, mt
short tons	9.078×10^{-1}	mt
oz mt^{-1}	3.43×10^{1}	parts per million, ppm
Velocity		
ft sec^{-1} (= ft/sec)	3.048×10^{-1}	m sec^{-1} (= m/sec)
mi hr^{-1}	1.6093	km hr^{-1}
mi hr^{-1}	4.470×10^{-1}	m sec^{-1}
Pressure, stress		
lb in^{-2} (= lb/in^2), psi	7.03×10^{-2}	kg cm^{-2} (= kg/cm^2)
lb in^{-2}	6.804×10^{-2}	atmospheres, atm
lb in^{-2}	6.895×10^{3}	newtons (N)/m^2, N m^{-2}
atm	1.0333	kg cm^{-2}
atm	7.6×10^{2}	mm of Hg (at 0° C)
inches of Hg (at 0° C)	3.453×10^{-2}	kg cm^{-2}
bars, b	1.020	kg cm^{-2}
b	1.0×10^{6}	dynes cm^{-2}
b	9.869×10^{-1}	atm
b	1.0×10^{-1}	megapascals, MPa
Density		
lb in^{-3} (= lb/in^3)	2.768×10^{1}	gr cm^{-3} (= gr/cm^3)
Viscosity		
poises	1.0	gr cm^{-1} sec^{-1} or dynes cm^{-2}
Discharge		
U.S. gal min^{-1}, gpm	6.308×10^{-2}	l sec^{-1}
gpm	6.308×10^{-5}	m^3 sec^{-1}
ft^3 sec^{-1}	2.832×10^{-2}	m^3 sec^{-1}
Hydraulic conductivity		
U.S. gal day^{-1} ft^{-2}	4.720×10^{-7}	m sec^{-1}
Permeability		
darcies	9.870×10^{-13}	m^2
Transmissivity		
U.S. gal day^{-1} ft^{-1}	1.438×10^{-7}	m^2 sec^{-1}
U.S. gal min^{-1} ft^{-1}	2.072×10^{-1}	l sec^{-1} m^{-1}
Magnetic field intensity		
gausses	1.0×10^{5}	gammas
Energy, heat		
British thermal units, BTU	2.52×10^{-1}	calories, cal
BTU	1.0758×10^{2}	kilogram-meters, kgm
BTU lb^{-1}	5.56×10^{-1}	cal kg^{-1}
Temperature		
°C + 273	1.0	°K (Kelvin)
°C + 17.78	1.8	°F (Fahrenheit)
°F − 32	5/9	°C (Celsius)

Divide by the factor number to reverse conversions.
Exponents: for example 4.047×10^{3} (see acres) = 4,047; 9.29×10^{-2} (see ft^2) = 0.0929.

Editor: Jiri Zidek
Drafter: Michael Wooldridge

Type face: Palatino

Presswork: Miehle Single Color Offset
Harris Single Color Offset

Binding: Saddlestitched with softbound cover

Paper: Cover on 12-pt. Kivar
Text on 70-lb White Matte

Ink: Cover—PMS 320
Text—Black

Quantity: 700